

# Endoplasmic Reticulum Stress Is Associated With Autophagy and Cardiomyocyte Remodeling in Experimental and Human Atrial Fibrillation

Marit Wiersma, PhD;\* Roelien A. M. Meijering, PhD;\* Xiao-Yan Qi, PhD; Deli Zhang, PhD; Tao Liu, MD; Femke Hoogstra-Berends, BSc; Ody C. M. Sibon, PhD; Robert H. Henning, MD, PhD; Stanley Nattel, MD; Bianca J. J. M. Brundel, PhD

**Background**—Derailment of proteostasis, the homeostasis of production, function, and breakdown of proteins, contributes importantly to the self-perpetuating nature of atrial fibrillation (AF), the most common heart rhythm disorder in humans. Autophagy plays an important role in proteostasis by degrading aberrant proteins and organelles. Herein, we investigated the role of autophagy and its activation pathway in experimental and clinical AF.

**Methods and Results**—Tachypacing of HL-1 atrial cardiomyocytes causes a gradual and significant activation of autophagy, as evidenced by enhanced LC3B-II expression, autophagic flux and autophagosome formation, and degradation of p62, resulting in reduction of Ca<sup>2+</sup> amplitude. Autophagy is activated downstream of endoplasmic reticulum (ER) stress: blocking ER stress by the chemical chaperone 4-phenyl butyrate, overexpression of the ER chaperone-protein heat shock protein A5, or overexpression of a phosphorylation-blocked mutant of eukaryotic initiation factor 2 $\alpha$  (eIF2 $\alpha$ ) prevents autophagy activation and Ca<sup>2+</sup>-transient loss in tachypaced HL-1 cardiomyocytes. Moreover, pharmacological inhibition of ER stress in tachypaced *Drosophila* confirms its role in derailing cardiomyocyte function. In vivo treatment with sodium salt of phenyl butyrate protected atrial-tachypaced dog cardiomyocytes from electrical remodeling (action potential duration shortening, L-type Ca<sup>2+</sup>-current reduction), cellular Ca<sup>2+</sup>-handling/contractile dysfunction, and ER stress and autophagy; it also attenuated AF progression. Finally, atrial tissue from patients with persistent AF reveals activation of autophagy and induction of ER stress, which correlates with markers of cardiomyocyte damage.

**Conclusions**—These results identify ER stress-associated autophagy as an important pathway in AF progression and demonstrate the potential therapeutic action of the ER-stress inhibitor 4-phenyl butyrate. (*J Am Heart Assoc.* 2017;6:e006458. DOI: 10.1161/JAHA.117.006458.)

**Key Words:** 4PBA • atrial fibrillation • autophagy • *Drosophila* • drug research • Endoplasmic Reticulum stress • HSPA5 • molecular biology • structural biology • tachypacing

Atrial fibrillation (AF) is the most common persistent clinical tachyarrhythmia.<sup>1</sup> Many patients experience clinical symptoms, including palpitations, fatigue, and weakness; AF also puts patients at risk for cardiac morbidity and mortality and often necessitates life-long anticoagulant therapy.<sup>1</sup> When AF persists, sinus rhythm (SR) reversion and maintenance becomes

progressively more difficult. Central to this self-perpetuating nature of AF is the remodeling of cardiomyocytes as a consequence of the increased atrial activation rate, resulting in disturbances of electrophysiological features and contraction and structural damage.<sup>2</sup> Therapeutic strategies that limit cardiomyocyte remodeling would improve the success of

From the Department of Physiology, Amsterdam Cardiovascular Sciences, VU University Medical Center, Amsterdam, The Netherlands (M.W., D.Z., B.J.J.M.B.); Department of Clinical Pharmacy and Pharmacology (M.W., R.A.M.M., D.Z., F.H.-B., R.H.H., B.J.J.M.B.) and Department of Cell Biology (O.C.M.S.), University Medical Center Groningen, University of Groningen, The Netherlands (M.W., R.A.M.M., D.Z., F.H.-B., R.H.H., B.J.J.M.B.); Department of Medicine, Montreal Heart Institute and Université de Montréal, the Department of Pharmacology and Therapeutics, McGill University, Montreal, Québec, Canada (X.-Y.Q., S.N.); Institute of Pharmacology, West German Heart and Vascular Center, Faculty of Medicine, University Duisburg-Essen, Duisburg, Germany (X.-Y.Q., S.N.); and Department of Cardiology, Renmin Hospital of Wuhan University, Wuhan, China (T.L.).

\*Dr Wiersma and Dr Meijering contributed equally to this work.

Accompanying Figures S1 through S11 and Videos S1 through S18 are available at <http://jaha.ahajournals.org/content/6/10/e006458.full#sec-34>.

**Correspondence to:** Bianca J. J. M. Brundel, PhD, Department of Physiology, De Boelelaan 1118, 1081 HV Amsterdam, The Netherlands. E-mail: b.brundel@vumc.nl

Received April 21, 2017; accepted August 28, 2017.

© 2017 The Authors. Published on behalf of the American Heart Association, Inc., by Wiley. This is an open access article under the terms of the Creative Commons Attribution-NonCommercial License, which permits use, distribution and reproduction in any medium, provided the original work is properly cited and is not used for commercial purposes.

## Clinical Perspective

### What Is New?

- Macroautophagy appears to constitute an important mechanism of atrial cardiomyocyte remodeling in atrial fibrillation (AF).
- Endoplasmic reticulum stress is the upstream pathway inducing autophagy in AF.
- Oral treatment with the chemical chaperone 4-phenyl butyrate inhibited endoplasmic reticulum stress and counteracted disease progression in a dog model of AF.

### What Are the Clinical Implications?

- Pharmacological inhibition of endoplasmic reticulum stress and downstream autophagy may offer novel therapeutic strategies to limit disease progression in clinical AF.
- The endoplasmic reticulum stress inhibitor 4-phenyl butyrate, which is already approved for clinical use in urea cycle disorders, offers an immediate candidate to test the concept in clinical AF.

cardioversion, but are unavailable.<sup>1</sup> To identify druggable targets, recent research is increasingly directed at uncovering the molecular mechanisms underlying atrial remodeling.

Derailment of proteostasis (ie, the homeostasis of protein production, function, and breakdown) contributes to cardiomyocyte remodeling and predisposes to AF in experimental models and patients with AF.<sup>3–6</sup> Among recently identified factors contributing to proteostasis derailment in AF is the activation of proteases that degrade contractile and structural proteins, including cardiac troponins and  $\alpha$ -tubulin, resulting in breakdown of the microtubule network and cardiomyocyte structural remodeling.<sup>3,4,7</sup> The importance of proper proteostasis is also revealed by the attenuation of cardiomyocyte remodeling and dysfunction as a consequence of induction of heat shock proteins (HSPs), whose chaperone function subserves correct folding and preservation of contractile proteins.<sup>8,9</sup>

Macroautophagy (hereafter “autophagy”) is critically involved in maintaining proteostasis.<sup>10</sup> Autophagy is an evolutionarily conserved protein-degradation pathway that removes damaged or expired proteins and organelles by sequestration in autophagosomes and subsequent lysosomal degradation.<sup>10,11</sup> Recent work shows that the mammalian target of rapamycin (mTOR) pathway<sup>12,13</sup> and endoplasmic reticulum (ER) stress response<sup>13,14</sup> can activate the autophagy-lysosome pathway, which plays a major role in the cardiac stress response.<sup>15</sup> Autophagy is widely involved as a cell-stress pathway, whose excessive activation triggers cardiac remodeling in response to degradation of essential proteins and organelles. Activation of autophagy in the heart is implicated in cardiac remodeling in mitral regurgitation<sup>16,17</sup> and cardiac hypertrophy.<sup>18,19</sup>

Herein, we report that activation of autophagy by upstream ER stress constitutes an important mechanism of cardiac remodeling in tachypaced atrial-derived cardiomyocytes, *Drosophila*, and dogs and in atrial biopsy specimens from patients with AF. We provide data to show that blocking ER stress, by the chemical chaperone 4-phenyl butyrate (4PBA), overexpression of the ER chaperone HSPA5, or mutant constructs of eIF2 $\alpha$ , inhibits activation of autophagy and thereby precludes electrical and contractile dysfunction in both in vitro and in vivo AF models. Thus, our study points to ER stress as a potential novel druggable target to attenuate cardiac remodeling in AF.

## Methods

### HL-1 Atrial Cardiomyocyte Cell Culture, Transfections, and Constructs

HL-1 atrial cardiomyocytes derived from adult mouse atria were obtained from Dr William Claycomb (Louisiana State University, New Orleans).<sup>20</sup> The cardiomyocytes were maintained in complete Claycomb Medium (Sigma) supplemented with 10% fetal bovine serum, 100 U/mL penicillin, 100  $\mu$ g/mL streptomycin, 4 mmol/L L-glutamine, 0.3 mmol/L L-ascorbic acid, and 100  $\mu$ mol/L norepinephrine. HL-1 cardiomyocytes were cultured on cell culture plastics or on glass coverslips coated with 0.02% gelatin in a humidified atmosphere of 5% CO<sub>2</sub> at 37°C. Where indicated, HL-1 cardiomyocytes were transiently transfected with the LC3B–green fluorescent protein (kind gift of Professor T. Johansen),<sup>21</sup> HSPA5 (kind gift of Professor H. Kampinga), pcDNA3.1<sup>+</sup> (empty), eIF2 $\alpha$  wild type, eIF2 $\alpha$  S51A, or eIF2 $\alpha$  S51D plasmid, by the use of Lipofectamine 2000.

### Tachypacing of HL-1 Cardiomyocytes and Calcium Transient Measurements

HL-1 cardiomyocytes were subjected to tachypacing, as described before.<sup>3</sup> In short, HL-1 cardiomyocytes were subjected to 1 Hz (normal pacing) or 6 Hz (tachypacing; Table 1), 40 V, and 20-millisecond pulses, for a maximal duration of 8 hours via the C-Pace EP Culture Stimulator. These frequencies were used to standardize the control firing frequency (1 Hz is the average spontaneous beating rate of HL-1 cardiomyocytes) and to produce a similar frequency increment with tachypacing (6-fold increase) to that which occurs during AF in humans. To measure Ca<sup>2+</sup> transients (CaTs), HL-1 cardiomyocytes were incubated for 30 minutes with 2  $\mu$ mol/L Ca<sup>2+</sup>-sensitive dye, Fluo-4-AM. Fluo-4–loaded cardiomyocytes were excited by a 488-nm laser with emission at 500 to 550 nm and were visually recorded with a 40 $\times$  objective, using a Solamere-Nipkow-Confocal-Live-Cell-Imaging system (based on a DM IRE2 inverted microscope). The live recording of CaT in HL-1 cardiomyocytes was

**Table 1.** Comparison of the Different Models Used

Model	NP Group, Hz (bpm)	TP Group, Hz (bpm)
HL-1	1 (60)	6 (360)
<i>Drosophila</i>	1.5 (90)	5 (300)
Dog	1.3 (80)	10 (600)*

Bpm indicates beats per minute; NP, normal-paced; and TP, tachypaced.

\*Please note that 600 bpm atrial tachypacing in the dog induces atrial fibrillation (AF), with atrial-tissue responses at  $\approx$ 6 to 8 Hz. This model is intentionally used to produce sustained AF, thereby mimicking the clinical situation.

performed at 1-Hz stimulation at 37°C. Live recordings were further processed by use of the software ImageJ. The relative value of fluorescence signals between experiments was determined using the following calibration:  $F_{cal} = F_1/F_0$ , where  $F_1$  is the fluorescent dye signal at any given time and  $F_0$  is the fluorescent signal at rest. Mean values and SEMs from each experimental condition were based on 7 consecutive CaTs in at least 50 cardiomyocytes.

## Drug Treatment

Pepstatin A, bafilomycin A1 (BAF), tunicamycin, rapamycin, and 4PBA were dissolved, according to manufacturer's instructions. HL-1 cardiomyocytes were treated with 4PBA (10 mmol/L), tunicamycin (5  $\mu$ g/mL), and rapamycin (50 nmol/L) 8 hours before pacing. Pepstatin A (10  $\mu$ mol/L) and BAF (10 nmol/L) were added 30 minutes before normal or tachypacing.

## Drosophila Stocks, Tachypacing, and Heart Wall Contraction Assays

For all experiments,  $w^{1118}$  strains were used. All flies were maintained at 25°C on standard medium. After fertilization, adult flies were removed and drugs were added to the medium containing fly embryos. *Drosophila* embryos and larvae were treated with 4PBA (100 mmol/L), pepstatin A (100  $\mu$ mol/L), or BAF (100 nmol/L) during development. Controls were treated with the vehicle, 2% dimethyl sulfoxide. After 2 days, prepupae were selected for tachypacing, as previously described.<sup>22</sup> Groups of at least 5 prepupae were subjected to tachypacing (5 Hz for 20 minutes, 20-V and 5-millisecond pulses; Table 1) with a C-Pace EP Culture Stimulator. Before and after tachypacing, videos of spontaneous heart wall contractions in whole prepupae were recorded for 30 seconds. Heart wall contractions were analyzed with IonOptix software.

## Western Blot Analysis

Western blot analysis was performed, as previously described.<sup>3</sup> Briefly, equal amounts of total protein in SDS-PAGE sample

buffer were separated on SDS-PAGE 4% to 20% Precise Tris-HEPES gels. After transfer to nitrocellulose membranes, membranes were incubated with primary antibodies, followed by incubation with horseradish peroxidase-conjugated anti-mouse or anti-rabbit secondary antibodies. Signals were detected by the Western Lightning Ultra method and quantified by densitometry via the software Gene Gnome, Gene tools. The following antibodies were purchased: rabbit anti-phosphorylated protein kinase B (Akt; Ser473), rabbit anti-Akt, rabbit anti-LC3B, rabbit anti-SQSTM1/p62, rabbit anti-phosphorylated eIF2 $\alpha$  (Ser51), rabbit anti-phosphorylated S6 ribosomal protein (Ser235/236), mouse anti-S6 ribosomal protein, rabbit anti-phosphorylated mTOR (Ser2448/2481), rabbit anti-mTOR, mouse anti-eIF2 $\alpha$ , mouse anti-HSPA5, mouse anti- $\beta$ -actin, and mouse anti-GAPDH; rabbit anti- $\beta$ -myosin heavy chain 7 (MHC) was a kind gift of Professor J. Van der Velden.

## Quantitative Real-Time Polymerase Chain Reaction

Total RNA was isolated from HL-1 cardiomyocytes using the nucleospin RNA isolation kit. First-strand cDNA was generated by M-MLV reverse transcriptase and random primers. Relative changes in transcription level were determined using the CFX384 Real-Time System C1000 Thermocycler in combination with SYBR green ROX-mix. Calculations were performed using the comparative threshold cycle method, according to User Bulletin 2. Fold inductions were adjusted for GAPDH levels.

Primer pairs used included the following: ATF4, GTCCGTTA-CAGCAACACTGC (forward) and CCACCATGGCGTATTAGAGG (reverse); ATF6, AAGAGAAGCCTGTCACTG (forward) and GGCTGGTAGTGTCTGAAT (reverse); CHOP, GACCAGTTCTGC TTTCAGG (forward) and CAGCGACAGAGCCAGAATAA (reverse); HSPA5, ATCTTTGGTTGCTTGCTGCT (forward) and ATGAAGGAGACTGCTGAGGC (reverse); autophagy gene 12, CTCCACAGCCCATTCTTTG (forward) and AACTCCCGGAGAC ACCAAG (reverse); and GAPDH, CATCAAGAAGGTGGTGAAGC (forward) and ACCACCCTGTTGCTGTAG (reverse). Polymerase chain reaction efficiencies for all primer pairs were between 90% and 110%.

## Immunofluorescent Staining and Confocal Analysis

HL-1 cardiomyocytes were untransfected or transiently transfected with green fluorescent protein-LC3B for 48 hours and paced at 1 Hz (normal pacing) or 6 Hz (tachypacing). This was followed by fixation with 4% formaldehyde for 15 minutes at room temperature and washing 3 times with PBS; then, they were permeabilized and blocked with 0.3% Triton X-100 and 5% fetal bovine serum in PBS (1 hour at room

temperature). Endogenous LC3B was visualized by the anti-LC3B antibody and a secondary Alexa-488-labeled anti-rabbit antibody; endogenous MHC was visualized by the anti-MHC (kind gift of Professor J. Van der Velden) and a secondary fluorescein isothiocyanate-labeled anti-rabbit antibody. Endogenous LC3B, green fluorescent protein–LC3B puncta, indicative of autophagosomes, and MHC were visualized by confocal microscopy and captured at  $\times 125$  magnification. The number of puncta was counted manually from at least 2 independent experiments using ImagePro. Mean values and SEMs from each experimental condition were based on at least 20 cardiomyocytes in case of transfection and at least 50 in case of drug treatment.

### In Vivo Dog Model for AF

Adult mongrel dogs were divided into 3 groups: nonpaced, atrial tachypaced (ATP; Table 1) to maintain AF, or ATP with sodium salt of PBA (Na-PBA) treatment (300 mg/kg per day, orally). All dogs underwent the same surgical procedure, AF induction measurements, and cardiomyocyte contractility and electrophysiological measurements. The dogs were anesthetized with acepromazine (0.07 mg/kg IM), ketamine (5.3 mg/kg IV), diazepam (0.25 mg/kg IV), and isoflurane (1.5%); then, they were intubated and ventilated. One bipolar pacing lead was fixed into the right atrial (RA) appendage via the left jugular vein under fluoroscopic guidance. The tip was connected to a programmable pacemaker. Results in 7 ATP dogs with Na-PBA were compared with 7 tachypaced dogs without treatment and 7 nonpaced control dogs. Na-PBA was given orally (300 mg/kg per day), starting 3 days before and continuing throughout ATP. For the ATP and ATP with Na-PBA groups, the pacemakers were turned on 24 hours after surgery to stimulate the RA at 600 beats per minute for 7 successive days. The ECG was checked daily to ensure AF during pacing. At the end of the study, all dogs were anesthetized with morphine (2 mg/kg SC) and  $\alpha$ -chloralose (120 mg/kg IV bolus, followed by 29.25 mg/kg per hour IV infusion); then, they were intubated and ventilated. Body temperature was maintained at 37°C. After midline sternotomy, the pericardium was opened and 2 bipolar electrodes were fixed to the RA appendage (1 for pacing and 1 for signal recording). For AF induction, the RA was paced at 50 Hz for 10 seconds. A total of 5 to 10 AF episodes were recorded to calculate the mean AF duration in each dog. An AF episode  $>10$  minutes was considered sustained, and the electrophysiological study was terminated. Cardioversion was avoided to prevent tissue damage, which precludes further cellular and molecular studies.

### Atrial Cardiomyocyte Isolation

After electrophysiological study, the heart was excised and immersed in oxygen-saturated Tyrode solution (in mmol/L):

NaCl 136, KCl 5.4, MgCl<sub>2</sub> 1, CaCl<sub>2</sub> 2, NaH<sub>2</sub>PO<sub>4</sub> 0.33, HEPES 5, and dextrose 10 (pH 7.35), by NaOH. The left atrium (LA) was isolated from the heart with an intact blood supply. The left circumflex coronary artery was cannulated and perfused with Ca<sup>2+</sup> (1.8 mmol/L), followed by Ca<sup>2+</sup>-free Tyrode solution perfusion for 10 minutes. All leaking branches were ligated. The tissue was then perfused with Ca<sup>2+</sup>-free Tyrode solution containing 150 U/mL collagenase and 0.1% BSA for 60 minutes. Digested LA tissue was harvested and carefully stirred. Isolated cells were centrifuged (500 rpm, 3 minutes) to separate cardiomyocytes from fibroblasts. Cardiomyocytes were stored in Tyrode solution containing 200  $\mu$ mol/L Ca<sup>2+</sup> for Ca<sup>2+</sup>-imaging studies.

### Cardiomyocyte Ca<sup>2+</sup> Imaging and Cellular Contractility Assessment

Isolated cardiomyocytes were stimulated at 1 Hz, and all measurements were performed at 35 $\pm$ 2°C. Cell-Ca<sup>2+</sup> recording was obtained, as previously described, with the use of Indo-1 AM.<sup>3,23</sup> Cells were exposed to UV light (wavelength, 340 nm), and the exposure was controlled with an electronic shutter to minimize photographic bleaching. Emitted light was reflected into a spectral separator, passed through parallel filters at 400 and 500 nm ( $\pm 10$  nm), detected by matched photomultiplier tubes, and electronically filtered at 60 Hz. Background fluorescence was removed by adjusting the 400- and 500-nm channels to 0 over an empty field of view near the cell. Fluorescence signal ratios (*R*) were recorded and converted to [Ca<sup>2+</sup>]<sub>i</sub> following the equation developed by Grynkiewicz et al<sup>24</sup>: [Ca<sup>2+</sup>]<sub>i</sub>=Kd $\beta$  [(*R*–*R*<sub>min</sub>)/(*R*<sub>max</sub>–*R*)], where  $\beta$  is the ratio of the 500-nm signals at low and saturating [Ca<sup>2+</sup>]<sub>i</sub>. Intracellular Kd for Indo-1 was 844 nm. Cell and sarcomere contractility was detected by automatic edge detection, and 5 successive beats were averaged for each measurement.

### Cell Electrophysiological Recordings

Borosilicate glass electrodes filled with pipette solution were connected to a patch-clamp amplifier. Electrodes had tip resistances of 2 to 4 M $\Omega$ . For perforated-patch recording, nystatin-free intracellular solution was placed in the tip of the pipette by capillary action ( $\approx 30$  seconds); then, pipettes were back-filled with nystatin-containing (600  $\mu$ g/mL) pipette solution. Data were sampled at 5 kHz and filtered at 1 kHz. Whole cell currents are expressed as densities (pA/pF). Junction potentials between bath and pipette solutions averaged 10.5 mV and were corrected for APs only. Tyrode solution contained the following (in mmol/L): NaCl 136, CaCl<sub>2</sub> 1.8, KCl 5.4, MgCl<sub>2</sub> 1, NaH<sub>2</sub>PO<sub>4</sub> 0.33, dextrose 10, and HEPES 5, titrated to pH 7.3 with NaOH. The pipette solution for AP

recording contained the following (mmol/L): GTP 0.1, potassium-aspartate 110, KCl 20, MgCl<sub>2</sub> 1, MgATP 5, HEPES 10, sodium-phosphocreatine 5, and EGTA 0.005 (pH 7.4, KOH). The extracellular solution for Ca<sup>2+</sup>-current measurement contained the following: tetraethylammonium chloride 136, CsCl 5.4, MgCl<sub>2</sub> 1, CaCl<sub>2</sub> 2, NaH<sub>2</sub>PO<sub>4</sub> 0.33, dextrose 10, and HEPES 5 (pH 7.4, CsOH). Niflumic acid (50 μmol/L) was added to inhibit Ca<sup>2+</sup>-dependent Cl current, and 4-aminopyridine (2 mmol/L) was added to suppress I<sub>to</sub>. The pipette solution for Ca<sup>2+</sup>-current recording contained the following (in mmol/L): CsCl 120, tetraethylammonium chloride 20, MgCl<sub>2</sub> 1, EGTA 10, MgATP 5, HEPES 10, and Li-GTP 0.1 (pH 7.4, CsOH).

## Patient Material

Before surgery, 1 investigator assessed patient characteristics (Table 2), as described before.<sup>7</sup> All patients were euthyroid and had normal left ventricular function. RA and LA appendages were obtained from all patients. After excision, the atrial appendages were immediately snap frozen in liquid nitrogen and stored at −85°C. The study conforms to the principles of the Declaration of Helsinki. The institutional review board approved the study, and patients gave written informed consent. Because of the low tissue yield per patient, not all experiments could be performed with each tissue sample. Therefore, at least 5 samples per group were used for experiments.

**Table 2.** Demographic and Clinical Characteristics of Patients With PeAF and Control Patients in SR

Characteristics	SR Group (n=17)	PeAF Group (n=28)
RAA	17 (100)	25 (89)
LAA	14 (82)	27 (96)
Age, mean±SEM, y	58±5	61±3
Duration of AF, median (range), mo	...	8 (0.1–56)
Underlying heart disease/surgical procedure		
Lone AF/maze	0 (0)	7 (25)*
CAD/MVI	17 (100)	21 (75)*
Medication		
Digoxin	1 (6)	13 (46) <sup>†</sup>
Calcium antagonists	9 (53)	10 (36)
Blockers	17 (100)	9 (32) <sup>‡</sup>

Values are represented as number (percentage) of patients unless otherwise indicated. AF indicates atrial fibrillation; CAD, coronary artery disease; LAA, left atrial appendage; maze, atrial arrhythmia surgery; MVI, mitral valve insufficiency; PeAF, persistent AF; RAA, right atrial appendage; and SR, sinus rhythm.

\**P*≤0.05, <sup>†</sup>*P*≤0.01, <sup>‡</sup>*P*≤0.001 vs SR.

## Statistical Analysis

Results are expressed as mean±SEM of at least 3 independent experiments. Statistical analysis was performed using a Student *t* test for single comparison between 2 groups. For analysis involving >2 groups, statistical comparison was performed using a 1-way ANOVA. When showing significance, individual group differences were assessed using a Bonferroni-corrected *t* test. Correlations were estimated using Pearson correlation and tested to be significantly nonzero using Pearson correlation tests. All *P* values were 2 sided. *P*≤0.05 was considered statistically significant. SPSS version 20 was used for all statistical evaluations.

## Results

### Tachypacing of Cardiomyocytes Induces Autophagy

To explore whether tachypacing induces autophagy, the autophagy markers p62 and LC3B were tested. P62 is sequestered to autophagosomes during autophagy and degraded on fusion with the lysosome; reduced levels of p62 are an indication of autophagic activation.<sup>25–27</sup> LC3B-II is a protein produced from LC3B-I on activation of autophagy and is also incorporated into autophagosomes; LC3B-II levels correlate with the induction of autophagy.<sup>25–27</sup> Tachypacing of HL-1 atrial cardiomyocytes, in which 8-hour tachypacing produces changes resembling those reported in persistent AF (PeAF) in humans,<sup>3,28</sup> activates autophagy, as demonstrated by a time-dependent decrease in the expression of p62 and increase in LC3B-II levels (Figure 1A through 1C). No such changes were noted in cardiomyocytes paced at 1 Hz (ie, their average intrinsic firing frequency; Figure S1). For the sake of clarity, results for normal-paced cardiomyocyte data shown in the figures without other specification were obtained after 8 hours of pacing. Furthermore, HL-1 atrial cardiomyocytes show normal morphological characteristics and are viable during normal pacing and tachypacing, as assessed by bright-field microscopy (Figure S2). Tachypacing also induces a clear redistribution of LC3B into discrete perinuclear puncta in both untransfected cardiomyocytes and LC3B–green fluorescent protein transfected cardiomyocytes (Figure 1D through 1F, Figure S3), supporting autophagosome formation.<sup>29</sup> Next, we determined the autophagic flux, to discriminate between the induction of autophagy and decreased degradation of autophagosomes, by blocking autophagosome-lysosome fusion with (Figure 1G and 1H).<sup>27,30</sup> BAF pretreatment further increases LC3B-II levels of tachypaced cardiomyocytes, but did not affect normal-paced cardiomyocytes (Figure 1G and 1H, Figures S4 and S5). This finding, together with reduced p62 levels,

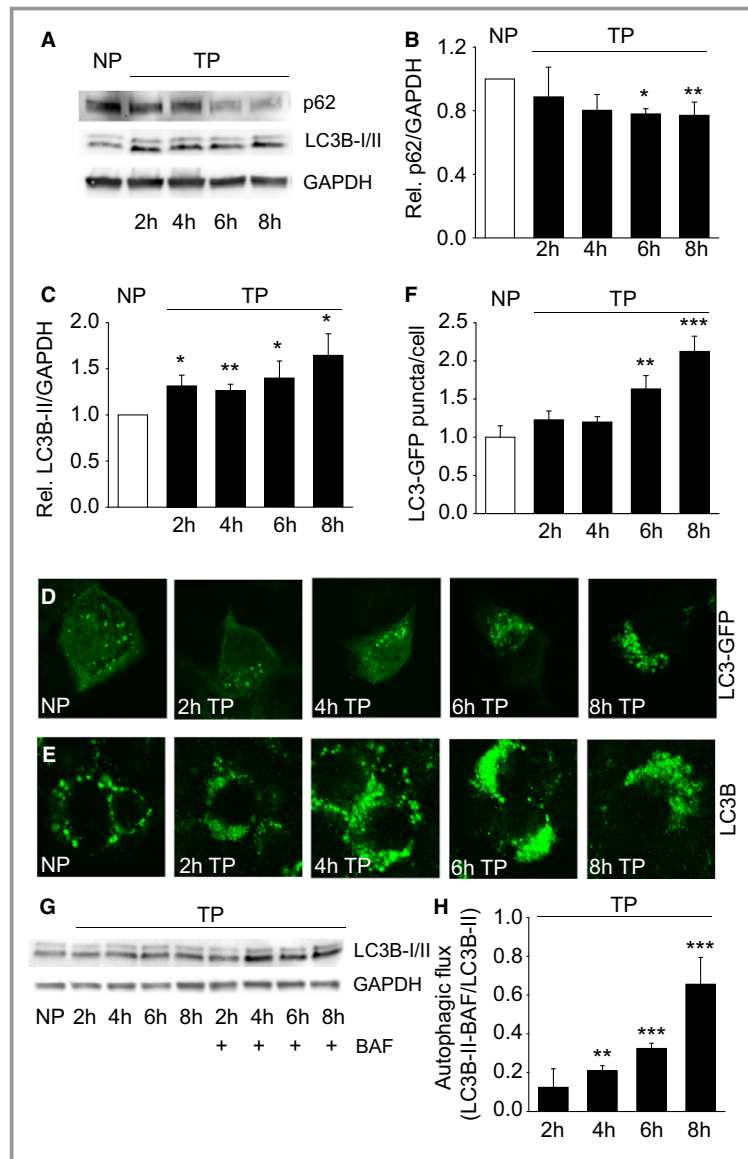


**Figure 1.** Tachypacing (TP) induces autophagosome formation and enhanced activation of TP-induced autophagy. A, Representative Western blot of TP-induced autophagy markers p62 (molecular weight [MW], 62), LC3B-I and LC3B-II (MWs, 14 and 16, respectively), and loading control GAPDH (MW, 37). HL-1 cardiomyocytes were normal paced (NP) or TP for the duration indicated. B, Quantified data showing a significant reduction in p62 levels after 6 or more hours of TP (N=4). C, Quantified data showing a significant increase in LC3B-II levels, beginning after 2 hours of TP (N=5). D, Confocal images of TP HL-1 cardiomyocytes, for the period as indicated, transfected with LC3B–green fluorescent protein (GFP) plasmid. E, Confocal images of TP HL-1 cardiomyocytes for the period as indicated. Endogenous LC3B was visualized by immunostaining. Green puncta indicate autophagosomes. F, Quantified data showing accumulation of LC3B-GFP punctae/cardiomyocytes during TP (n/N=35/3). G, Representative Western blot of HL-1 cardiomyocytes NP vs TP for the duration, as indicated, in the presence or absence of bafilomycin A1 (BAF). H, Quantification of the autophagic flux by determining the difference in LC3B-II levels in the presence vs absence of BAF (N=4). Note that all NP data are shown after 8 hours of observation. \* $P \leq 0.05$ , \*\* $P \leq 0.01$ , \*\*\* $P \leq 0.001$  vs NP.

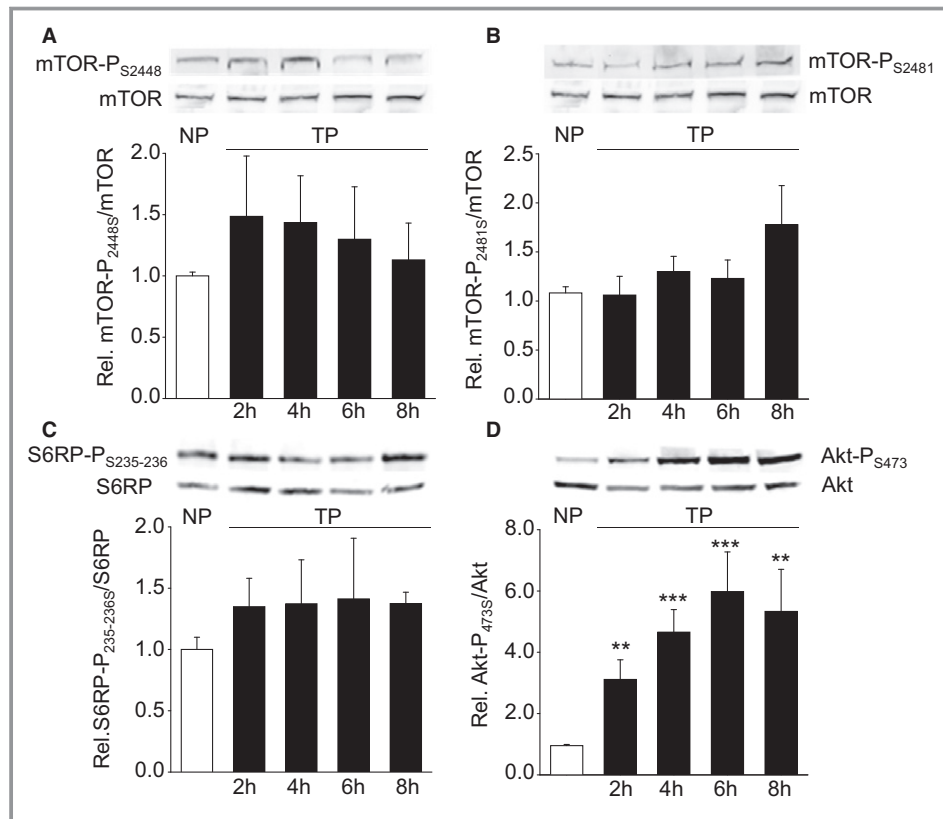


**Figure 2.** Tachypacing (TP)-induced autophagy does not involve mammalian target of rapamycin complex (mTORC) signaling. Top panels: Western blots of proteins within mTORC signaling. Bottom panels: Quantified data of the ratio of phosphorylated proteins normalized for basal protein levels. Phosphorylated mTOR S2448 (mTORC1; molecular weight [MW], 289; N=3; A), phosphorylated mTOR S2481 (mTORC2; MW, 289; N=3; B), phosphorylated ribosomal protein S6 (S6RP) S235/236 (downstream of mTORC1; MW, 32; N=3; C), and phosphorylated protein kinase B (Akt) S473 (downstream of mTORC2 and endoplasmic reticulum stress; MW, 60; N=3; D) in response to TP for the duration, as indicated, compared with normal pacing (NP). Note that all NP data shown are after 8 hours of observation. \*\* $P < 0.01$ , \*\*\* $P < 0.001$  vs NP.

indicates that tachypacing increases functional autophagic activity in HL-1 atrial cardiomyocytes.

### ER Stress Is Associated With Autophagy in a Tachypaced Cardiomyocyte Model

To investigate which upstream pathway activates autophagy, we first examined the mTOR. mTOR assembles into 2 complexes, mTOR complex (mTORC) 1 and mTORC2; both complexes become activated by mTOR phosphorylation, although at different sites, after which they attenuate autophagy.<sup>12,31</sup> To test whether tachypacing-induced autophagy results from the inhibition of mTOR signaling, we determined total mTOR, phosphorylation of mTOR at S2448 for mTORC1 and S2481 for mTORC2, and their respective downstream targets, ribosomal protein S6 and Akt (Figure 2A through 2D). Tachypacing does not affect phosphorylation of

mTOR at S2448 or S2481; it also does not affect phosphorylation of the mTORC1 downstream effector ribosomal protein S6 at S235/S236. However, tachypacing significantly increases phosphorylation of Akt at S473 (Figure 2D). Given the increased Akt phosphorylation, which is independent of mTORC2, we next examined involvement of ER stress signaling in tachypacing-induced autophagic flux; Akt S473 phosphorylation is observed during ER stress,<sup>32</sup> and ER stress is an important regulator of autophagy.<sup>14</sup> A role of ER stress was suggested by the finding that tachypacing strongly increases phosphorylation of its downstream effector eIF2 $\alpha$  (Figure 3A and 3B, Figure S6), which, on phosphorylation, induces transcription of ER stress and autophagy genes (ie, *ATF4*, *ATF6*, *CHOP*, *HSPA5*, and *ATG12*; Figure 3C). In addition, tachypacing gradually induced protein levels of HSPA5 (Figure S7), an endogenous ER chaperone-protein induced by ER stress.<sup>33</sup> These results suggest that ER stress

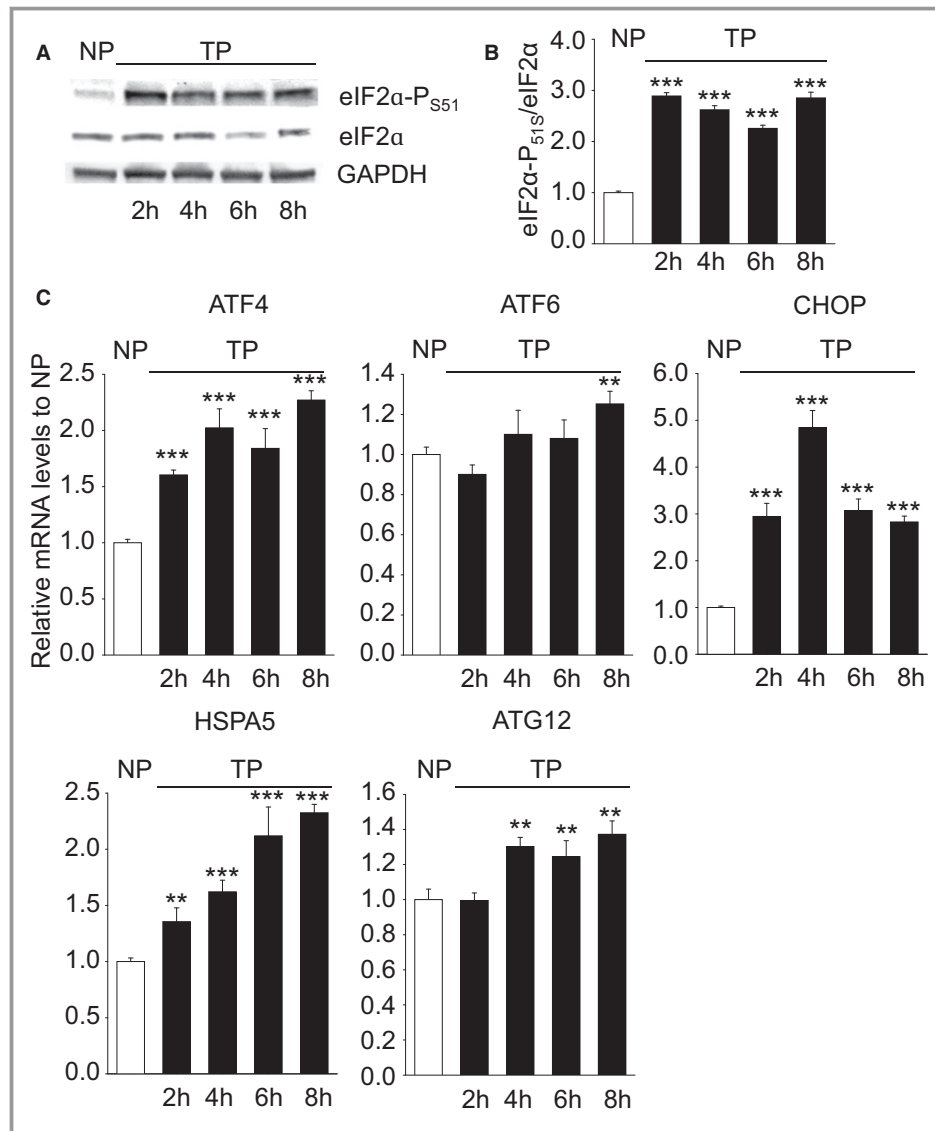


**Figure 3.** Tachypacing (TP) augments levels of endoplasmic reticulum (ER) stress markers and the autophagy gene *ATG12*. A, Representative Western blot of phosphorylated eIF2 $\alpha$  S51 (molecular weight [MW], 38), an ER stress marker, basal eIF2 $\alpha$  (MW, 36), and GAPDH levels during normal pacing (NP) or in response to TP for the indicated duration. B, Quantified data of the ratio of phosphorylated eIF2 $\alpha$  S51 normalized for basal eIF2 $\alpha$  protein levels (N=3). C, Quantitative real-time polymerase chain reaction of ER stress markers ATF4, ATF6, CHOP, and heat shock protein (HSP) A5 and the autophagy-related gene *ATG12* in response to TP for the indicated duration relative to NP (N=3). Note that all NP data shown are after 8 hours of observation. \*\* $P \leq 0.01$ , \*\*\* $P \leq 0.001$  vs NP.

is the upstream activator of autophagy in the tachypaced cardiomyocyte model.

To extend the findings to human AF, we examined autophagy, ER stress, and markers of cardiac remodeling in atrial appendages of patients with PeAF along with control patients in SR. Patients with PeAF showed an accumulation of autophagosomes and autolysosomes and the presence of myolysis (degradation of sarcomeres) on electron microscopic examination, which is absent in patients in SR (Figure 4A

through 4D).<sup>34</sup> Autophagy is further evidenced in patients with AF by enhanced LC3B-II induction and decreased levels of p62 compared with patients in SR (Figure 4E). The ER stress chaperone-protein HSPA5 showed a trend towards increased expression in patients with PeAF compared with patients in SR. Previously, we reported on structural remodeling involving degradation of contractile proteins in these patients.<sup>4,7</sup> Involvement of autophagy in structural remodeling and AF progression is substantiated by the correlation of p62



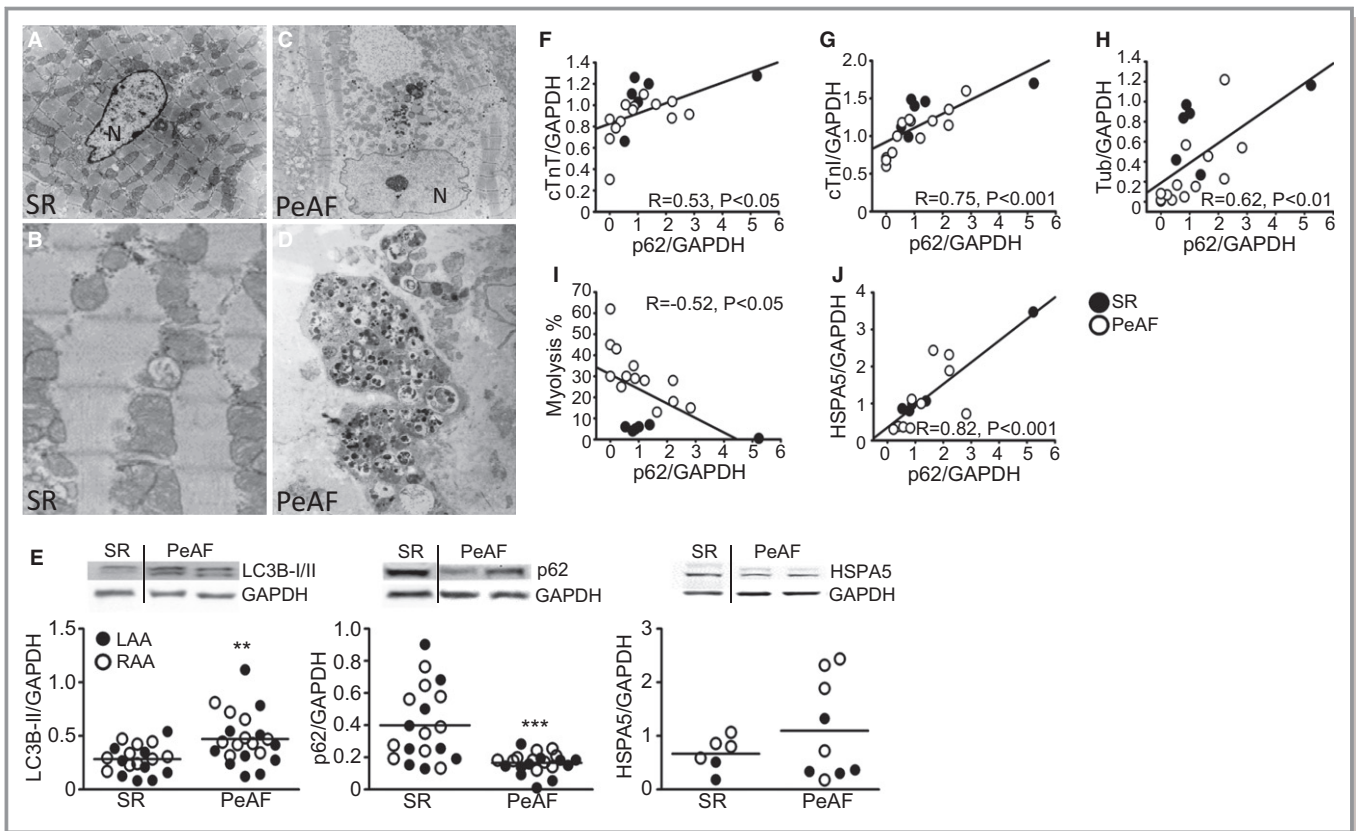


**Figure 4.** Patients with persistent atrial fibrillation (PeAF) show markers of endoplasmic reticulum (ER) stress and autophagy. A, Electron microscopic image of left atrial appendage (LAA) of a patient in sinus rhythm (SR), showing normal sarcomere structures and absence of autophagosomes and autolysosomes. B, Image of LAA of a patient in SR, showing normal sarcomere structures and absence of perinuclear autophagosomes and autolysosomes at higher magnification. C, Electron microscopic image of LAA of a patient with PeAF, which shows the presence of autophagosomes and autolysosomes with an electron-dense core with a perinuclear (N) localization. D, Image of LAA of a patient with PeAF at a higher magnification, showing the presence of autophagosomes and autolysosomes. E, Top panel: Representative Western blot of the autophagy markers LC3B-II and p62 and the ER stress chaperone-protein heat shock protein (HSP) A5 in atrial appendages of patients with PeAF vs those in SR. Bottom panel: Quantified data of the autophagy markers LC3B-II and p62 and the ER stress chaperone-protein HSPA5 in atrial appendages of patients with PeAF vs those in SR. F through J, Significant correlations between levels of the autophagy marker p62 and markers of cardiomyocyte structural remodeling in patients with PeAF and patients in SR. F, Cardiac troponin T (cTnT). G, Cardiac troponin I (cTnI). H,  $\alpha$ -Tubulin (Tub). I Myolysis. J, HSPA5. RAA indicates right atrial appendage. \*\* $P \leq 0.01$ , \*\*\* $P \leq 0.001$  vs SR.

expression with cardiac troponins (I and T) and  $\alpha$ -tubulin expression in patients with PeAF and those in SR (Figure 4F through 4H); there was an inverse correlation with the amount of myolysis (Figure 4I). Levels of p62 also correlated with HSPA5 levels (Figure 4J), suggesting that an ER stress response is associated with autophagy and AF progression. Although 1 data point seems to be an outlier, statistical analysis showed it did not qualify as such. Nevertheless, to exclude undue influence of this data point on correlations, we have repeated the analyses, omitting this data point. For most analyses, correlation remained statistically significant, with the exception of cardiac troponin T and myolysis (Figure 4F:  $R=0.43$ ,  $P=0.075$ ; Figure 4G:  $R=0.74$ ,  $P<0.001$ ; Figure 4H:  $R=0.49$ ,  $P<0.05$ ; Figure 4I:  $R=-0.46$ ,  $P=0.056$ ; Figure 4J:  $R=0.62$ ,  $P<0.05$ ).

The correlation of autophagy markers with degradation of contractile proteins and the amount of structural remodeling suggest a biologically relevant contribution of this pathway to AF-induced derailment of cardiomyocyte proteostasis and disease progression.

### Inhibition of ER Stress Attenuates Autophagy and Protects From Cardiac Remodeling

The contribution of AF-induced ER stress and the subsequent enhanced autophagic flux to derailment of cardiomyocyte proteostasis and disease progression was tested by pharmacological and genetic manipulations in experimental model systems for AF. The orphan drug, 4PBA, in clinical use to treat urea cycle disorders,<sup>35–37</sup> has recently been recognized as an

inhibitor of ER stress by virtue of its chemical chaperone properties.<sup>38,39</sup> To explore its potential as a therapeutic agent in AF, we examined its properties in tachypaced cardiomyocytes, *Drosophila*, and a dog model of AF.

In tachypaced HL-1 cardiomyocytes, 4PBA limits ER stress and prevents activation of autophagy, as demonstrated by normalization of phosphorylated eIF2 $\alpha$  expression and LC3B-II and attenuation of p62 breakdown (Figure 5A and 5B). In addition, 4PBA treatment prevents tachypacing-induced accumulation of the contractile protein MHC in perinuclear puncta in HL-1 cardiomyocytes (Figure 5C and 5D). The protective 4PBA effects are mediated via upstream ER stress inhibition, because downstream inhibition of the autophagic process by pepstatin A (a lysosomal cathepsin D/E inhibitor) or BAF (a lysosomal fusion inhibitor) attenuated p62 degradation but did not normalize the phosphorylation of eIF2 $\alpha$ , LC3B-II expression, and the formation of perinuclear MHC puncta on tachypacing (Figure 5A through 5D).

Next, we determined whether ER stress results in tachypacing-induced contractile dysfunction. HL-1 cardiomyocytes were pretreated with 4PBA, which caused protection against loss of CaTs in 8-hour tachypaced cardiomyocytes (Figure 5E and 5F, Figure S8A and S8B, Videos S1 through S4). Similar protective effects against CaT loss were observed in tachypaced HL-1 cardiomyocytes overexpressing the endogenous ER chaperone-protein HSPA5, indicating that ER stress is involved in contractile dysfunction (Figure 5G and 5H, Videos S5 through S8). To directly assess whether ER stress is associated with autophagy and contractile dysfunction, HL-1 cardiomyocytes were transfected with eIF2 $\alpha$  mutants (wild type, constitutively phosphorylated [S51D], or constitutively nonphosphorylated [S51A]), followed by tachypacing. Tachypaced HL-1 cardiomyocytes overexpressing the nonphosphorylated eIF2 $\alpha$  mutant were protected from CaT loss, in contrast to cardiomyocytes overexpressing the wild-type or constitutively phosphorylated eIF2 $\alpha$  mutants (Figure 5I and 5J). Normal-paced HL-1 cardiomyocytes, transfected with the eIF2 $\alpha$  mutants, showed no differences in CaT amplitude compared with nontransfected cardiomyocytes (Figure S8C and S8D). The findings indicate that activation of the ER stress pathway is an important modulator of contractile dysfunction. In addition, inhibition of autophagic flux by preincubating HL-1 cardiomyocytes with the autophagy inhibitors pepstatin A and BAF was also protective against tachypacing-induced CaT loss. This again emphasized the role of ER stress-associated autophagy in contractile function (Figure 5E and 5F, Figure S8A and S8B, Videos S9 through S12). Pepstatin A and BAF effects are not conveyed via indirect modulation of ER stress, because neither of the drugs influenced HSPA5 expression levels, as suggested before (Figure S9).<sup>40</sup>

To extend these findings to a multicellular experimental animal model for tachypacing-induced contractile dysfunction,

similar experiments were conducted in *Drosophila*.<sup>3,22</sup> Comparable to findings in tachypaced HL-1 cardiomyocytes, inhibition of ER stress (4PBA) and autophagy (BAF) attenuates tachypacing-induced dysfunction in heart wall contractions in *Drosophila* (Figure 5K and 5L, Videos S13 through S18), whereas pepstatin A is not protective and toxic at the concentrations applied. Moreover, activators of ER stress (tunicamycin) and autophagy (rapamycin) resulted in ER stress and contractile dysfunction in tachypaced HL-1 cardiomyocytes and *Drosophila* (Figure S10).

## ER Stress Attenuation Relieves Autophagy and Protects From Cardiac Remodeling in an in Vivo Animal Model

To obtain proof of concept that ER stress is involved in AF promotion in a large animal model for AF, dogs were subjected to 7 days of ATP (equal to persistent human AF<sup>41</sup>), to induce AF-associated atrial remodeling, and were treated with the orally administered Na-PBA (300 mg/kg per day). In isolated atrial cardiomyocytes, Na-PBA treatment protects from tachypacing-induced electrical changes, including shortening of action potential duration and reductions in L-type Ca<sup>2+</sup> channel current (Figure 6A and 6B). In addition, Na-PBA treatment prevents tachypacing-induced abnormalities in Ca<sup>2+</sup> handling and associated hypocontractility of isolated atrial cardiomyocytes (Figure 6C through 6F). Finally, Na-PBA conserved the effective refractory period at various sites at both RA and LA and significantly attenuated the vulnerability to AF induction (Figure 6G and 6H). In addition, the protective effect of Na-PBA was not via modulation of HDAC activity, because HDAC levels were not altered by Na-PBA treatment, as has been suggested before (Figure S11).<sup>42</sup> Furthermore, Na-PBA reduces markers of ER stress and autophagy in LA tissue of tachypaced dogs, as demonstrated by an increase in p62 level and reductions in LC3B-II and HSPA5 levels compared with nontreated tachypaced dogs (Figure 7A through 7C). Moreover, Na-PBA treatment protected against MHC reduction in tachypaced dogs (Figure 7D), suggesting that attenuation of ER stress results in conservation of contractile protein expression.

Thus, tachypacing induces ER stress-triggered autophagic flux, which plays a prominent role in cardiomyocyte remodeling and AF progression (Figure 8).<sup>43</sup> Findings from a clinically relevant dog model for AF indicate that the chemical chaperone 4PBA protects the heart against AF, making 4PBA a potentially interesting drug candidate for treating clinical AF.

## Discussion

In the current study, we report that ER stress-associated enhanced autophagic flux appears to constitute an important

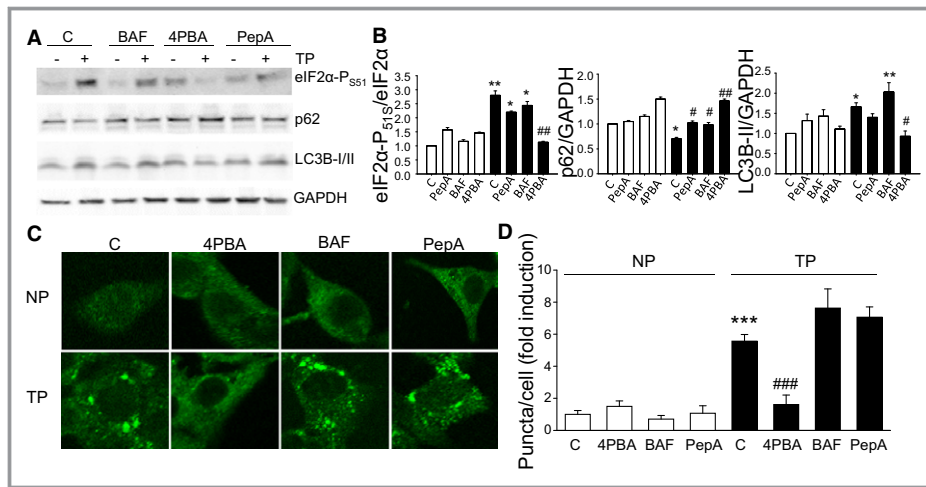


**Figure 5.** Inhibition of endoplasmic reticulum (ER) stress and autophagy protects against tachypacing (TP)-induced contractile dysfunction in HL-1 cardiomyocytes and *Drosophila melanogaster*. A, Representative Western blot of ER stress marker (eIF2 $\alpha$ -PS51) and autophagy markers (LC3B-II and p62) in HL-1 cardiomyocytes pretreated with dimethyl sulfoxide (DMSO; control [C]), the autophagy modulator pepstatin A (PepA) or bafilomycin A1 (BAF), or the molecular chaperone 4-phenyl butyrate (4PBA). B, Quantified data showing that HL-1 cardiomyocytes treated with 4PBA reveal attenuation of TP-induced increase in eIF2 $\alpha$ -PS51, LC3B-II induction, and reduction in p62. PepA and BAF inhibit lysosomal cathepsin D/E and lysosomal fusion, respectively, and therefore result in an induction of LC3B-II levels and attenuation of p62 reduction without affecting upstream eIF2 $\alpha$ -PS51 levels. Open bars represent normal-paced (NP) cardiomyocytes, whereas closed bars represent TP cardiomyocytes after 8 hours of observation. N=3. C, Confocal images of NP and TP HL-1 cardiomyocytes after 8 hours of observation, stained for myosin heavy chain with DMSO (C), 4PBA, BAF, or PepA pretreatment. D, Quantified data showing the number of puncta for the conditions as indicated, all obtained after 8 hours of observation. 4PBA pretreatment protects against the formation of perinuclear puncta (n/N=60/3). E, Representative Ca<sup>2+</sup> transients (CaT; 5 seconds) of HL-1 cardiomyocytes after NP or TP. HL-1 cardiomyocytes were pretreated with the autophagy modulators PepA or BAF, or the chemical chaperone 4PBA, followed by NP or TP and measurement of CaT. F, Quantified CaT amplitude of HL-1 cardiomyocytes after NP or TP (n/N=60/4). HL-1 cardiomyocytes were pretreated with the autophagy modulators PepA or BAF or the ER chaperone 4PBA. G, Representative CaT (5 seconds) of HL-1 cardiomyocytes transfected with empty plasmid (C) or ER chaperone heat shock protein (HSP) A5, followed by NP or TP. H, Quantified CaT amplitude of NP and TP HL-1 cardiomyocytes transiently transfected with empty plasmid or HSPA5 (n/N=30/3). I, Representative CaT (5 seconds) of HL-1 cardiomyocytes transfected with empty plasmid (C), eIF2 $\alpha$  wild-type, nonphosphorylated (S52A), or phosphorylated mimetic (S52D) mutant and followed by NP or TP. J, Quantified CaT amplitude of NP and TP cardiomyocytes transiently transfected with empty plasmid (C), eIF2 $\alpha$  wild-type, constitutively nonphosphorylated (S52A), or constitutively phosphorylated (S52D) mutant (n/N=30/3). K, Representative heart wall contractions of *Drosophila* monitored before TP (sinus rhythm [SR]) and after TP with DMSO (C) or PepA, BAF, or 4PBA pretreatment. L, Quantified data showing heart wall contraction rates of *Drosophila* before and after TP with DMSO (C) or PepA, BAF, or 4PBA treatment. Open bars represent NP (in HL-1 cardiomyocytes) or spontaneous heart rate (SR; in *Drosophila*), and closed bars represent TP HL-1 cardiomyocytes or *Drosophila*. N=9 to 15 prepupae for each group. Note that all NP data shown are after 8 hours of observation. \* $P \leq 0.05$ , \*\* $P \leq 0.01$ , \*\*\* $P \leq 0.001$  vs control NP or before TP; # $P \leq 0.05$ , ## $P \leq 0.01$ , ### $P \leq 0.001$  vs control (after) TP.

mechanism of cardiac remodeling in tachypaced cardiomyocytes, *Drosophila*, dogs, and atrial biopsy specimens from patients with AF. We provide data to show that blocking ER stress, by the chemical chaperone 4PBA, or overexpressing a

phosphorylation-blocked mutant of eIF2 $\alpha$  inhibits activation of autophagy and, thereby, suppresses cardiomyocyte remodeling in both in vitro and in vivo AF models. Thus, our study points to ER stress as a potential novel druggable target for

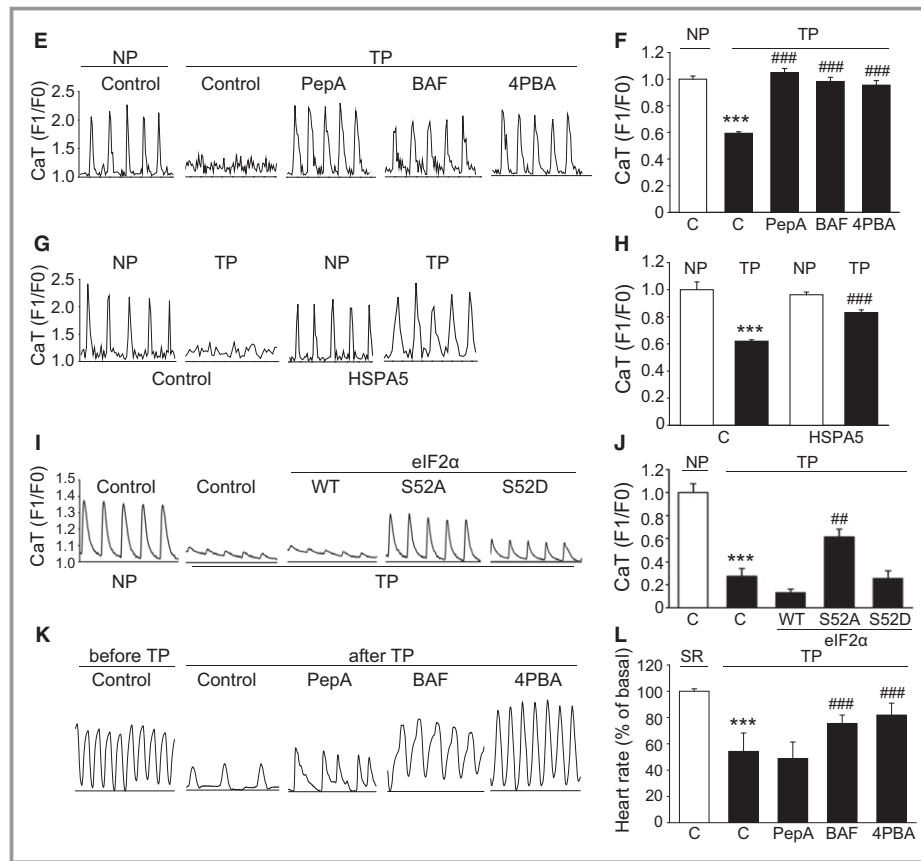


Figure 5. Continued.

cardiac remodeling in AF and proposes that 4PBA may emerge as a novel lead compound for the development of agents to attenuate AF progression.

### Prominent Role of ER Stress–Associated Autophagy in Cardiomyocyte Remodeling

Although it is recognized that the increased atrial activation rate constitutes a major driving force for cardiac remodeling in AF,<sup>1</sup> molecular events leading to remodeling have been poorly identified. We examined both experimental and clinical AF models that equal persistent human AF, which show reversible electrical and irreversible structural remodeling.<sup>3,8,28,44,45</sup> We were able to reveal a prominent role for ER stress–associated enhanced autophagic flux in cardiomyocyte remodeling and AF progression using various pharmacological and genetic manipulations of the ER stress pathway (Figure 8). First, tachypacing-induced contractile dysfunction of HL-1 cardiomyocytes coincided with activation of known key players of this pathway. These include both phosphorylation of the ER stress regulator eIF2α at S51 and downstream expression of the stress-responsive transcripts ATF4 and ATF6. In turn, ATF4 and ATF6 activate autophagy,<sup>10</sup> via

enhanced expression of CHOP and the autophagy genes *ATG12* and *LC3B*, resulting in the elongation of autophagosomes and a sustained and excessive autophagic flux, as observed in tachypaced HL-1 cardiomyocytes.<sup>12,46–48</sup> Second, our data demonstrate that induction of ER stress represents the upstream event in tachypacing-elicited contractile-protein accumulation and contractile dysfunction. Genetic overexpression of a phosphorylation-blocked eIF2α protein or the ER chaperone HSPA5 abrogated both autophagy and contractile dysfunction. Knockdown of autophagy genes, such as *ATG5* or *ATG7*, was avoided because of the detrimental effects in healthy cardiomyocytes.<sup>15,49–51</sup> A prominent role for ER stress–induced autophagy in AF promotion is supported by pharmacological interventions. We observed that inhibition of the autophagic process by pepstatin A (a lysosomal cathepsin D/E inhibitor) or BAF (a lysosomal fusion inhibitor) protected against contractile dysfunction, but did not prevent the ER stress response and accumulation of contractile proteins within the HL-1 cardiomyocytes. Pharmacological prevention of ER stress by the chemical chaperone 4PBA precluded ER stress–related autophagy and cardiac remodeling in tachypaced HL-1 cardiomyocytes and *Drosophila*, as well as in the tachypaced dog model of AF-associated remodeling. Finally,

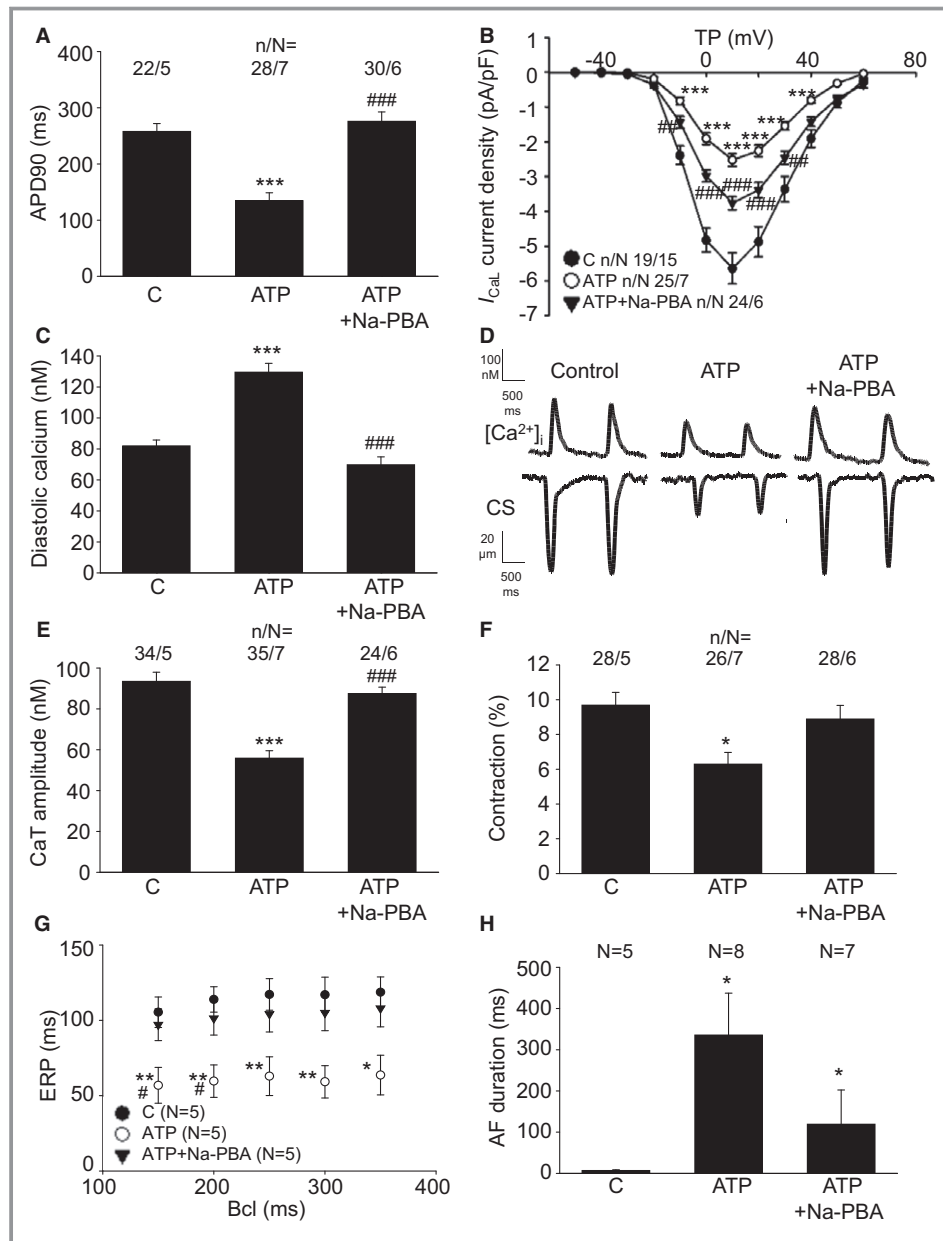


**Figure 6.** Sodium salt of phenyl butyrate (Na-PBA) protects against atrial remodeling in a dog model for atrial fibrillation (AF). Atrial tachypacing (ATP) induces atrial remodeling, measured as shortening of action potential duration (APD90; A), reduced L-type  $Ca^{2+}$  current ( $I_{CaL}$ ; B), and increased diastolic calcium levels in cardiomyocytes (n=15–40 cardiomyocytes; C). D, Representative calcium transient (CaT) and cell shortening (CS) tracers for the conditions, as indicated. Furthermore, ATP results in loss of CaT amplitude (E), loss of contractility (F), reduced adaptation of the effective refractory period (ERP) at different basic cycle lengths (BCLs; G), and increased duration of induced AF (H). All ATP-induced atrial remodeling end points were significantly attenuated by Na-PBA treatment. C indicates control. \* $P \leq 0.05$ , \*\* $P \leq 0.01$ , \*\*\* $P \leq 0.001$  vs C; # $P \leq 0.05$ , ## $P \leq 0.01$ , ### $P \leq 0.001$  vs ATP.

ER stress and autophagy are also activated in clinical AF, as evidenced by the presence of autophagosomes and autolysosomes in atrial heart tissue, enhanced LC3B-II expression, and reduction in p62 levels in patients with PeAF. Although altered proteasome function can influence p62 expression,<sup>52</sup>

proteasome function is not altered in AF,<sup>7</sup> suggesting that the reduction in p62 levels is a consequence of autophagic flux activation. Although there is only a trend towards an increase in HSPA5 expression in patients with AF, diminished protein synthesis or enhanced degradation, by either the

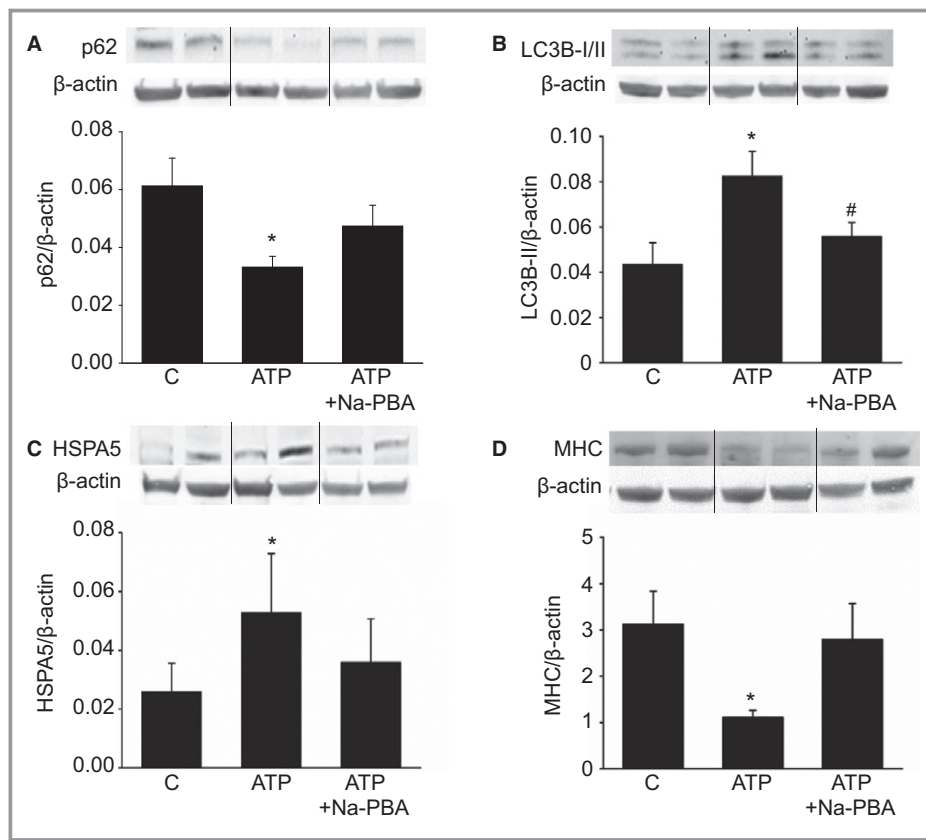


**Figure 7.** Sodium salt of phenyl butyrate (Na-PBA) protects against endoplasmic reticulum stress and autophagy in a dog model for atrial fibrillation. A, Top panel: Representative Western blot. Bottom panel: Quantified data revealing a significant reduction in p62 levels in atrial tachypacing (ATP), which was not significantly reduced by Na-PBA treatment compared with control (C) dogs. B, Representative Western blot of LC3B-I/II and loading control  $\beta$ -actin (molecular weight [MW], 43) in groups, as indicated. ATP causes significant induction in LC3B-II levels, which was significantly reduced in case of Na-PBA treatment. C, Representative Western blot of heat shock protein (HSP) A5, showing a trend ( $P=0.058$ ) in induction of HSPA5, which was not altered in Na-PBA-treated group. D, Representative Western blot of myosin heavy chain (MHC; MW, 230) in groups, as indicated. ATP causes a significant reduction in MHC, which was not changed in case of Na-PBA treatment. N=7 dogs for each group. \* $P\leq 0.05$  vs C, # $P\leq 0.05$  vs ATP.

proteasome or autophagy, or exhaustion of the protein levels may be the underlying cause.<sup>53</sup> There is ongoing debate about whether autophagy plays a beneficial or detrimental role in cardiac diseases.<sup>54,55</sup> Excessive autophagy contributed to age-related cardiac disease development, including heart failure, hypertension-induced cardiac diseases, mitral regurgitation, and diabetic cardiomyopathy.<sup>16,19,56–58</sup> Interestingly, all these cardiac diseases are recognized to represent a substrate for AF,<sup>59</sup> suggesting a role for autophagic activation in AF development. This is supported by the presence of autophagosome accumulation in patients who developed postoperative AF.<sup>60</sup> On the other hand, in inherited cardiomyopathies, autophagic activation was found to be beneficial.<sup>61–63</sup> In inherited cardiomyopathies, proteotoxic mutant proteins are likely cleared by autophagy. This

assumption is strengthened by a study showing that autophagy could be induced as a cellular defense mechanism against ER stress-mediated cell death by degrading protein aggregates.<sup>14</sup> Hence, it is clear that autophagic activation in the diverse cardiac diseases is not uniform in its function, but depends on the origin of cardiac disease; it can have either a beneficial (inherited cardiomyopathies) or detrimental (age-related cardiac diseases) effect on the course and outcome of the disease. Because protein aggregation has not been observed in most age-related cardiac diseases, including AF,<sup>55</sup> our findings suggest that the autophagic machinery becomes overengaged with maladaptive consequences, possibly because of divergent  $\text{Ca}^{2+}$  handling in the ER. The ER plays a prominent role in proper cell function, because at least one third of all proteins are synthesized in this organelle. ER

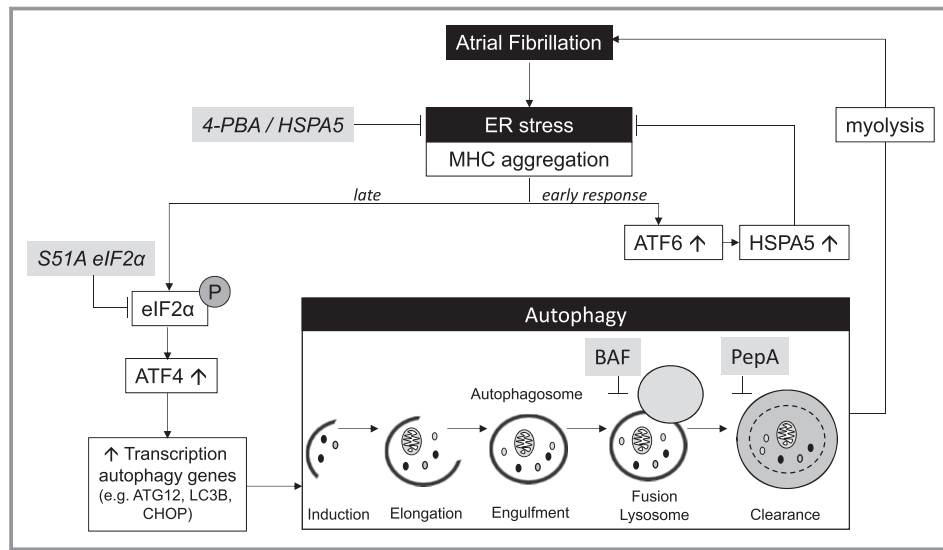


**Figure 8.** Proposed model for the role of autophagy and disease progression in atrial fibrillation (AF). AF triggers endoplasmic reticulum (ER) stress in cardiomyocytes, followed by the ER stress response, which results in activation of ATF6 and upregulation of heat shock protein (HSP) A5 expression in an attempt to restore ER homeostasis. ER stress then activates downstream phosphorylation of eIF2 $\alpha$ .<sup>4,3</sup> In turn, this results in the activation of the transcription factor ATF4, which regulates the expression of autophagy genes and LC3B, causing activation of autophagy by stimulating induction and elongation of autophagosomes. Initially, AF-induced activation of autophagy may preserve cardiomyocyte proteostasis; however, excessive stress-induced autophagy contributes to loss of contractile function and cardiac remodeling. ER stress-induced autophagy appears maladaptive, because inhibition of autophagy via 4-phenyl butyrate (4PBA), HSPA5, or nonphosphorylatable mutant eIF2 $\alpha$  (S51A) overexpression, pepstatin A (PepA), and bafilomycin A1 (BAF) prevented AF-associated remodeling and progression in our studies. MHC indicates  $\beta$ -myosin heavy chain 7.

chaperone proteins, especially HSPA5, assist in the correct folding of the newly formed proteins.<sup>64</sup> Reduced levels of HSPA5, or calcium overload in the ER, cause proteins to unfold and produce an ER stress response.<sup>65,66</sup> Because calcium overload plays a central role in experimental and clinical AF progression<sup>6,67–69</sup> and the ER is an important organelle to buffer calcium, calcium overload is a plausible trigger for ER stress, as observed in the current study. Further experimental confirmation of the role of ER calcium loading in inducing the AF-related stress response is of interest. Although our data demonstrate that (upstream) blockade of ER stress, by 4PBA or a phosphorylation-blocked eIF2 $\alpha$  mutant, prevents progression of AF, (downstream) blockade of autophagy elicited a similar effect, suggesting that activation of autophagy mediates cardiomyocyte remodeling in AF. In addition to clearance of damaged proteins, the generation of adenosine triphosphate for the cardiomyocyte is an important function of autophagy.<sup>70</sup> It is known that AF results in depletion of adenosine triphosphate levels. Cardiomyocytes may compensate for energy loss by generating adenosine triphosphate via autophagy at the expense of degradation of sarcomeric proteins (myolysis), as observed in experimental and clinical AF.<sup>4,7</sup>

## Therapeutic Implications

From a translational perspective, the current results identify a potential benefit of pharmacological inhibition of ER stress as a therapeutic strategy in clinical AF. Among the available compounds, 4PBA seems promising, because this compound is already approved for clinical use to treat urea cycle disorders<sup>36,37,71</sup> and is available under the trade names Buphenyl (available in the United States since 1996) and Ammonaps (available in Europe since 1999). 4PBA acts as a chemical chaperone and alleviates ER stress by protecting from aggregation of misfolded proteins. There are several ongoing human trials with 4PBA, which target ER stress in various clinical diseases featuring protein misfolding, including amyotrophic lateral sclerosis (NCT00107770), Huntington disease (NCT00212316), spinal muscular atrophy (NCT00528268), proteinuric nephropathies (NCT02343094), and cystic fibrosis (NCT00016744). Data from patients with urea cycle disorders to date indicate that 4PBA is safe and displays minor adverse effects,<sup>35</sup> although conventional dosing is high (maximum, 20 g/d). In addition, our results indicate that cardiac remodeling in AF may also be modulated by inhibitors of autophagy.<sup>47,72,73</sup> However, treatment with autophagy

inhibitors may precipitate considerable toxicity, as reported for bafilomycin,<sup>74</sup> or additional detrimental effects because of disruption of normal cell physiological characteristics by inhibition of basal autophagy.<sup>15,17,75,76</sup> Application of inhibitors of autophagy in AF and other chronic conditions thus awaits development of selective inhibitors targeting excessive autophagy. On the basis of these considerations, 4PBA may serve as a useful compound to explore the benefits of repression of ER stress-associated autophagy in the attenuation of AF progression and improvement of cardioversion outcome in clinical AF. 4PBA may serve as a lead compound for the further development of autophagy inhibitors for clinical use.

## Limitations

HL-1 atrial cardiomyocytes are derived from mouse atria and generally show similar features as adult cardiomyocytes.<sup>20</sup> Despite potential differences, the ease of confirmation of specific molecular pathways conferring tachypaced-induced remodeling by use of genetic manipulation is an important advantage of the HL-1 model. Moreover, findings in the tachypaced HL-1 atrial cardiomyocyte model have been confirmed repeatedly in the tachypaced dog model and clinical human AF.<sup>3,8</sup> Therefore, the tachypaced HL-1 model has merit to identify potential signaling pathways involved in AF remodeling.

The patient groups differed in terms of medications prescribed, as expected on the basis of the different disease causes of each group. For example, patients with AF frequently received digoxin for rate control, whereas patients in SR almost never took digoxin. On the other hand, patients in SR requiring surgery for coronary artery disease, like our control group, almost always receive  $\beta$  blockers, whereas a minority of patients with PeAF take them for rate control. Adjustments for these differences in our overall population cannot be made because of too few individuals; effects of drugs may also differ between SR and PeAF populations. Nevertheless, changes in patient data were similar to those observed in the in vitro HL-1 atrial cardiomyocyte model and the in vivo dog model.

## Sources of Funding

This study was supported by the Dutch Heart Foundation (2013T096 and 2013T144), LSH-Impulse grant (40-43100-98-008), The Netherlands Cardiovascular Research Initiative, Dutch Heart Foundation CVON2014-40 DOSIS and CVON-STW2016-14728 AFFIP, NWO VICI grant (865.10.012 to Sibon), and the Canadian Institutes of Health Research (Foundation grant). Nattel received support from the Quebec Heart and Stroke Foundation.

## Disclosures

None.

## References

- Dobrev D, Carlsson L, Nattel S. Novel molecular targets for atrial fibrillation therapy. *Nat Rev Drug Discov*. 2012;11:275–291.
- de Groot NM, Houben RP, Smeets JL, Boersma E, Schotten U, Schalij MJ, Crijns H, Allessie MA. Electropathological substrate of longstanding persistent atrial fibrillation in patients with structural heart disease: epicardial breakthrough. *Circulation*. 2010;122:1674–1682.
- Zhang D, Wu CT, Qi X, Meijering RA, Hoogstra-Berends F, Tadevosyan A, Cubukcuoglu Deniz G, Durdu S, Akar AR, Sibon OC, Nattel S, Henning RH, Brundel BJ. Activation of histone deacetylase-6 induces contractile dysfunction through derailment of alpha-tubulin proteostasis in experimental and human atrial fibrillation. *Circulation*. 2014;129:346–358.
- Brundel BJ, Ausma J, van Gelder IC, Van der Want JJ, van Gilst WH, Crijns HJ, Henning RH. Activation of proteolysis by calpains and structural changes in human paroxysmal and persistent atrial fibrillation. *Cardiovasc Res*. 2002;54:380–389.
- Ausma J, van der Velden HM, Lenders MH, van Ankeren EP, Jongsma HJ, Ramaekers FC, Borgers M, Allessie MA. Reverse structural and gap-junctional remodeling after prolonged atrial fibrillation in the goat. *Circulation*. 2003;107:2051–2058.
- Qi XY, Yeh YH, Xiao L, Burstein B, Maguy A, Chartier D, Villeneuve LR, Brundel BJ, Dobrev D, Nattel S. Cellular signaling underlying atrial tachycardia remodeling of L-type calcium current. *Circ Res*. 2008;103:845–854.
- Ke L, Qi XY, Dijkhuis AJ, Chartier D, Nattel S, Henning RH, Kampinga HH, Brundel BJ. Calpain mediates cardiac troponin degradation and contractile dysfunction in atrial fibrillation. *J Mol Cell Cardiol*. 2008;45:685–693.
- Brundel BJ, Shiroshita-Takeshita A, Qi X, Yeh YH, Chartier D, van Gelder IC, Henning RH, Kampinga HH, Nattel S. Induction of heat shock response protects the heart against atrial fibrillation. *Circ Res*. 2006;99:1394–1402.
- Ke L, Meijering RA, Hoogstra-Berends F, Mackovicova K, Vos MJ, Van Gelder IC, Henning RH, Kampinga HH, Brundel BJ. HSPB1, HSPB6, HSPB7 and HSPB8 protect against RhoA GTPase-induced remodeling in tachypaced atrial myocytes. *PLoS ONE*. 2011;6:e20395.
- Kroemer G, Marino G, Levine B. Autophagy and the integrated stress response. *Mol Cell*. 2010;40:280–293.
- Yang Z, Klionsky DJ. Eaten alive: a history of macroautophagy. *Nat Cell Biol*. 2010;12:814–822.
- Jung CH, Ro SH, Cao J, Otto NM, Kim DH. mTOR regulation of autophagy. *FEBS Lett*. 2010;584:1287–1295.
- He C, Klionsky DJ. Regulation mechanisms and signaling pathways of autophagy. *Annu Rev Genet*. 2009;43:67–93.
- Kouroku Y, Fujita E, Tanida I, Ueno T, Isoai A, Kumagai H, Ogawa S, Kaufman RJ, Kominami E, Momoi T. ER stress (PERK/eIF2alpha phosphorylation) mediates the polyglutamine-induced LC3 conversion, an essential step for autophagy formation. *Cell Death Differ*. 2007;14:230–239.
- Nakai A, Yamaguchi O, Takeda T, Higuchi Y, Hikoso S, Taniike M, Omiya S, Mizote I, Matsumura Y, Asahi M, Nishida K, Hori M, Mizushima N, Otsu K. The role of autophagy in cardiomyocytes in the basal state and in response to hemodynamic stress. *Nat Med*. 2007;13:619–624.
- Chen MC, Chang JP, Wang YH, Liu WH, Ho WC, Chang HW. Autophagy as a mechanism for myolysis of cardiomyocytes in mitral regurgitation. *Eur J Clin Invest*. 2011;41:299–307.
- Gurusamy N, Das DK. Is autophagy a double-edged sword for the heart? *Acta Physiol Hung*. 2009;96:267–276.
- Zhu H, Tannous P, Johnstone JL, Kong Y, Shelton JM, Richardson JA, Le V, Levine B, Rothermel BA, Hill JA. Cardiac autophagy is a maladaptive response to hemodynamic stress. *J Clin Invest*. 2007;117:1782–1793.
- Wiersma M, Henning RH, Brundel BJ. Derailed proteostasis as a determinant of cardiac aging. *Can J Cardiol*. 2016;11:1166.
- Claycomb WC, Lanson NA Jr, Stallworth BS, Egeland DB, Delcarpio JB, Bahinski A, Izzo NJ Jr. HL-1 cells: a cardiac muscle cell line that contracts and retains phenotypic characteristics of the adult cardiomyocyte. *Proc Natl Acad Sci USA*. 1998;95:2979–2984.
- Pankiv S, Clausen TH, Lamark T, Brech A, Bruun JA, Outzen H, Overvatn A, Bjorkoy G, Johansen T. p62/SQSTM1 binds directly to Atg8/LC3 to facilitate degradation of ubiquitinated protein aggregates by autophagy. *J Biol Chem*. 2007;282:24131–24145.

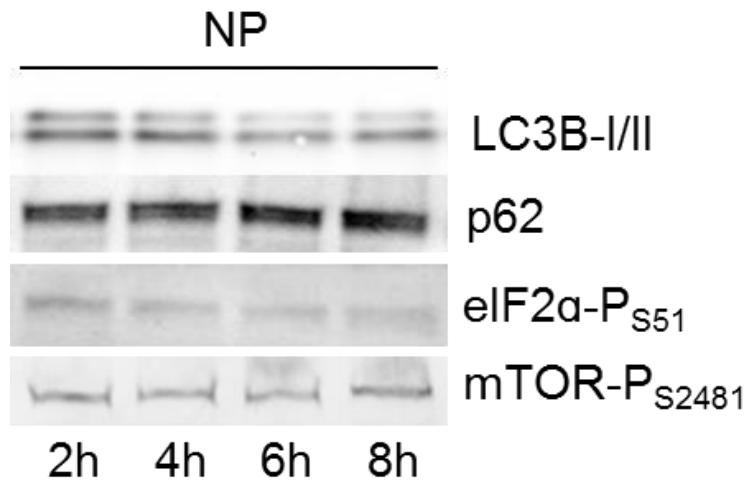


22. Zhang D, Ke L, Mackovicova K, Van Der Want JJ, Sibon OC, Tanguay RM, Morrow G, Henning RH, Kampinga HH, Brundel BJ. Effects of different small HSPB members on contractile dysfunction and structural changes in a *Drosophila melanogaster* model for atrial fibrillation. *J Mol Cell Cardiol*. 2011;51:381–389.
23. Brundel BJ, Henning RH, Ke L, van Gelder IC, Crijns HJ, Kampinga HH. Heat shock protein upregulation protects against pacing-induced myolysis in HL-1 atrial myocytes and in human atrial fibrillation. *J Mol Cell Cardiol* 2006;41:555–562.
24. Gryniewicz G, Poenie M, Tsien RY. A new generation of Ca<sup>2+</sup> indicators with greatly improved fluorescence properties. *J Biol Chem*. 1985;260:3440–3450.
25. Wang QJ, Ding Y, Kohtz DS, Mizushima N, Cristea IM, Rout MP, Chait BT, Zhong Y, Heintz N, Yue Z. Induction of autophagy in axonal dystrophy and degeneration. *J Neurosci*. 2006;26:8057–8068.
26. Maejima Y, Kyo S, Zhai P, Liu T, Li H, Ivessa A, Sciarretta S, Del Re DP, Zablocki DK, Hsu CP, Lim DS, Isobe M, Sadoshima J. Mst1 inhibits autophagy by promoting the interaction between Beclin1 and Bcl-2. *Nat Med*. 2013;19:1478–1488.
27. Klionsky DJ, Abdelmohsen K, Abe A, et al. Guidelines for the use and interpretation of assays for monitoring autophagy (3rd edition). *Autophagy*. 2016;12:1–222.
28. Brundel BJ, Kampinga HH, Henning RH. Calpain inhibition prevents pacing-induced cellular remodeling in a HL-1 myocyte model for atrial fibrillation. *Cardiovasc Res*. 2004;62:521–528.
29. Gottlieb RA, Mentzer RM. Autophagy during cardiac stress: joys and frustrations of autophagy. *Annu Rev Physiol*. 2010;72:45–59.
30. Hansen TE, Johansen T. Following autophagy step by step. *BMC Biol*. 2011;9:39.
31. Gurusamy N, Das DK. Detection of cell death by autophagy. *Methods Mol Biol*. 2009;559:95–103.
32. Yung HW, Charnock-Jones DS, Burton GJ. Regulation of AKT phosphorylation at Ser473 and Thr308 by endoplasmic reticulum stress modulates substrate specificity in a severity dependent manner. *PLoS ONE*. 2011;6:e17894.
33. Lee AS. The ER chaperone and signaling regulator GRP78/BiP as a monitor of endoplasmic reticulum stress. *Methods*. 2005;35:373–381.
34. Boyle AJ, Shih H, Hwang J, Ye J, Lee B, Zhang Y, Kwon D, Jun K, Zheng D, Sievers R, Angeli F, Yeghiazarians Y, Lee R. Cardiomyopathy of aging in the mammalian heart is characterized by myocardial hypertrophy, fibrosis and a predisposition towards cardiomyocyte apoptosis and autophagy. *Exp Gerontol*. 2011;46:549–559.
35. Carducci MA, Gilbert J, Bowling MK, Noe D, Eisenberger MA, Sinibaldi V, Zabelina Y, Chen TL, Grochow LB, Donehower RC. A phase I clinical and pharmacological evaluation of sodium phenylbutyrate on a 120-h infusion schedule. *Clin Cancer Res*. 2001;7:3047–3055.
36. Kibleur Y, Dobbelaere D, Barth M, Brassier A, Guffon N. Results from a Nationwide Cohort Temporary Utilization Authorization (ATU) survey of patients in France treated with Pheburane<sup>®</sup> (sodium phenylbutyrate) taste-masked granules. *Paediatr Drugs*. 2014;16:407–415.
37. Berry SA, Lichter-Konecki U, Diaz GA, McCandless SE, Rhead W, Smith W, Lemons C, Nagamani SC, Coakley DF, Mokhtarani M, Scharschmidt BF, Lee B. Glycerol phenylbutyrate treatment in children with urea cycle disorders: pooled analysis of short and long-term ammonia control and outcomes. *Mol Genet Metab*. 2014;112:17–24.
38. Kolb PS, Ayaub EA, Zhou W, Yum V, Dickhout JG, Ask K. The therapeutic effects of 4-phenylbutyric acid in maintaining proteostasis. *Int J Biochem Cell Biol*. 2015;61:45–52.
39. Cuadrado-Tejedor M, Ricobaraza AL, Torrijo R, Franco R, Garcia-Osta A. Phenylbutyrate is a multifaceted drug that exerts neuroprotective effects and reverses the Alzheimer's disease-like phenotype of a commonly used mouse model. *Curr Pharm Des*. 2013;19:5076–5084.
40. Ryter SW, Cloonan SM, Choi AM. Autophagy: a critical regulator of cellular metabolism and homeostasis. *Mol Cells*. 2013;36:7–16.
41. Li D, Fareh S, Leung TK, Nattel S. Promotion of atrial fibrillation by heart failure in dogs: atrial remodeling of a different sort. *Circulation*. 1999;100:87–95.
42. Mimori S, Ohtaka H, Koshikawa Y, Kawada K, Kaneko M, Okuma Y, Nomura Y, Murakami Y, Hamana H. 4-Phenylbutyric acid protects against neuronal cell death by primarily acting as a chemical chaperone rather than histone deacetylase inhibitor. *Bioorg Med Chem Lett*. 2013;23:6015–6018.
43. Hetz C, Chevet E, Oakes SA. Proteostasis control by the unfolded protein response. *Nat Cell Biol*. 2015;17:829–838.
44. Brundel BJ, Melnyk P, Rivard L, Nattel S. The pathology of atrial fibrillation in dogs. *J Vet Cardiol*. 2005;7:121–129.
45. Yang Z, Shen W, Rottman JN, Wikswo JP, Murray KT. Rapid stimulation causes electrical remodeling in cultured atrial myocytes. *J Mol Cell Cardiol*. 2005;38:299–308.
46. Hayashi-Nishino M, Fujita N, Noda T, Yamaguchi A, Yoshimori T, Yamamoto A. A subdomain of the endoplasmic reticulum forms a cradle for autophagosome formation. *Nat Cell Biol*. 2009;11:1433–1437.
47. Fleming A, Noda T, Yoshimori T, Rubinsztein DC. Chemical modulators of autophagy as biological probes and potential therapeutics. *Nat Chem Biol*. 2011;7:9–17.
48. Verfaillie T, Salazar M, Velasco G, Agostinis P. Linking ER stress to autophagy: potential implications for cancer therapy. *Int J Cell Biol*. 2010;2010:930509.
49. Gammoh N, Lam D, Puente C, Ganley I, Marks PA, Jiang X. Role of autophagy in histone deacetylase inhibitor-induced apoptotic and nonapoptotic cell death. *Proc Natl Acad Sci U S A*. 2012;109:6561–6565.
50. Li S, Liu C, Gu L, Wang L, Shang Y, Liu Q, Wan J, Shi J, Wang F, Xu Z, Ji G, Li W. Autophagy protects cardiomyocytes from the myocardial ischaemia-reperfusion injury through the clearance of CLP36. *Open Biol*. 2016;6:10.
51. Taneike M, Yamaguchi O, Nakai A, Hikoso S, Takeda T, Mizote I, Oka T, Tamai T, Oyabu J, Murakawa T, Nishida K, Shimizu T, Hori M, Komuro I, Takuji Shirasawa TS, Mizushima N, Otsu K. Inhibition of autophagy in the heart induces age-related cardiomyopathy. *Autophagy*. 2010;6:600–606.
52. Myeku N, Figueiredo-Pereira ME. Dynamics of the degradation of ubiquitinated proteins by proteasomes and autophagy: association with sequestosome 1/p62. *J Biol Chem*. 2011;286:22426–22440.
53. Rosengren V, Johansson H, Lehtio J, Fransson L, Sjöholm A, Orsater H. Thapsigargin down-regulates protein levels of GRP78/BiP in INS-1E cells. *J Cell Biochem*. 2012;113:1635–1644.
54. Delbridge LM, Mellor KM, Taylor DJ, Gottlieb RA. Myocardial stress and autophagy: mechanisms and potential therapies. *Nat Rev Cardiol*. 2017;14:412–425.
55. Henning RH, Brundel BJ. Proteostasis in cardiac health and disease. *Nat Rev Cardiol*. Jun 29, 2017. DOI: 10.1038/nrcardio.2017.89. Available at: ????. Accessed ??? ???, ???.
56. Tham YK, Bernardo BC, Ooi JY, Weeks KL, McMullen JR. Pathophysiology of cardiac hypertrophy and heart failure: signaling pathways and novel therapeutic targets. *Arch Toxicol*. 2015;89:1401–1438.
57. Ghavami S, Cunnington RH, Gupta S, Yeganeh B, Filomeno KL, Freed DH, Chen S, Klonisch T, Halayko AJ, Ambrose E, Singal R, Dixon IM. Autophagy is a regulator of TGF-beta1-induced fibrogenesis in primary human atrial myofibroblasts. *Cell Death Dis*. 2015;6:e1696.
58. Saito T, Asai K, Sato S, Hayashi M, Adachi A, Sasaki Y, Takano H, Mizuno K, Shimizu W. Autophagic vacuoles in cardiomyocytes of dilated cardiomyopathy with initially decompensated heart failure predict improved prognosis. *Autophagy*. 2016;12:579–587.
59. Andrade J, Khairy P, Dobrev D, Nattel S. The clinical profile and pathophysiology of atrial fibrillation: relationships among clinical features, epidemiology, and mechanisms. *Circ Res*. 2014;114:1453–1468.
60. Garcia L, Verdejo HE, Kuzmick J, Zalaquett R, Gonzalez S, Lavandero S, Corbalan R. Impaired cardiac autophagy in patients developing postoperative atrial fibrillation. *J Thorac Cardiovasc Surg*. 2012;143:451–459.
61. Choi JC, Muchir A, Wu W, Iwata S, Homma S, Morrow JP, Worman HJ. Temsirolimus activates autophagy and ameliorates cardiomyopathy caused by lamin A/C gene mutation. *Sci Transl Med*. 2012;4:144ra102.
62. Pattison JS, Robbins J. Protein misfolding and cardiac disease: establishing cause and effect. *Autophagy*. 2008;4:821–823.
63. Pattison JS, Osinska H, Robbins J. Atg7 induces basal autophagy and rescues autophagic deficiency in CryABR120G cardiomyocytes. *Circ Res*. 2011;109:151–160.
64. Diaz-Villanueva JF, Diaz-Molina R, Garcia-Gonzalez V. Protein folding and mechanisms of proteostasis. *Int J Mol Sci*. 2015;16:17193–17230.
65. Ribeiro CM, McKay RR, Hosoki E, Bird GS, Putney JW Jr. Effects of elevated cytoplasmic calcium and protein kinase C on endoplasmic reticulum structure and function in HEK293 cells. *Cell Calcium*. 2000;27:175–185.
66. Bertolotti A, Zhang Y, Hendershot LM, Harding HP, Ron D. Dynamic interaction of BiP and ER stress transducers in the unfolded-protein response. *Nat Cell Biol*. 2000;2:326–332.
67. Ausma J, Dispersyn GD, Duimel H, Thone F, Ver Donck L, Allessie MA, Borgers M. Changes in ultrastructural calcium distribution in goat atria during atrial fibrillation. *J Mol Cell Cardiol*. 2000;32:355–364.
68. Brundel BJ, van Gelder IC, Henning RH, Tuinenburg AE, Deelman LE, Tieleman RG, Grandjean JG, van Gilst WH, Crijns HJ. Gene expression of proteins influencing the calcium homeostasis in patients with persistent and paroxysmal atrial fibrillation. *Cardiovasc Res*. 1999;42:443–454.
69. Greiser M, Lederer WJ, Schotten U. Alterations of atrial Ca<sup>2+</sup> handling as cause and consequence of atrial fibrillation. *Cardiovasc Res*. 2011;89:722–733.

70. Ravikumar B, Futter M, Jahreiss L, Korolchuk VI, Lichtenberg M, Luo S, Massey DC, Menzies FM, Narayanan U, Renna M, Jimenez-Sanchez M, Sarkar S, Underwood B, Winslow A, Rubinsztein DC. Mammalian macroautophagy at a glance. *J Cell Sci.* 2009;122:1707–1711.
71. Schonthal AH. Targeting endoplasmic reticulum stress for cancer therapy. *Front Biosci (Schol Ed).* 2012;4:412–431.
72. Balgi AD, Fonseca BD, Donohue E, Tsang TC, Lajoie P, Proud CG, Nabi IR, Roberge M. Screen for chemical modulators of autophagy reveals novel therapeutic inhibitors of mTORC1 signaling. *PLoS ONE.* 2009;4:e7124.
73. Sciarretta S, Zhai P, Volpe M, Sadoshima J. Pharmacological modulation of autophagy during cardiac stress. *J Cardiovasc Pharmacol* 2012;60:235–241.
74. Drose S, Altendorf K. Bafilomycins and concanamycins as inhibitors of V-ATPases and P-ATPases. *J Exp Biol.* 1997;200:1–8.
75. Hara T, Nakamura K, Matsui M, Yamamoto A, Nakahara Y, Suzuki-Migishima R, Yokoyama M, Mishima K, Saito I, Okano H, Mizushima N. Suppression of basal autophagy in neural cells causes neurodegenerative disease in mice. *Nature.* 2006;441:885–889.
76. Maruyama R, Goto K, Takemura G, Ono K, Nagao K, Horie T, Tsujimoto A, Kanamori H, Miyata S, Ushikoshi H, Nagashima K, Minatoguchi S, Fujiwara T, Fujiwara H. Morphological and biochemical characterization of basal and starvation-induced autophagy in isolated adult rat cardiomyocytes. *Am J Physiol Heart Circ Physiol.* 2008;295:H1599–H1607.

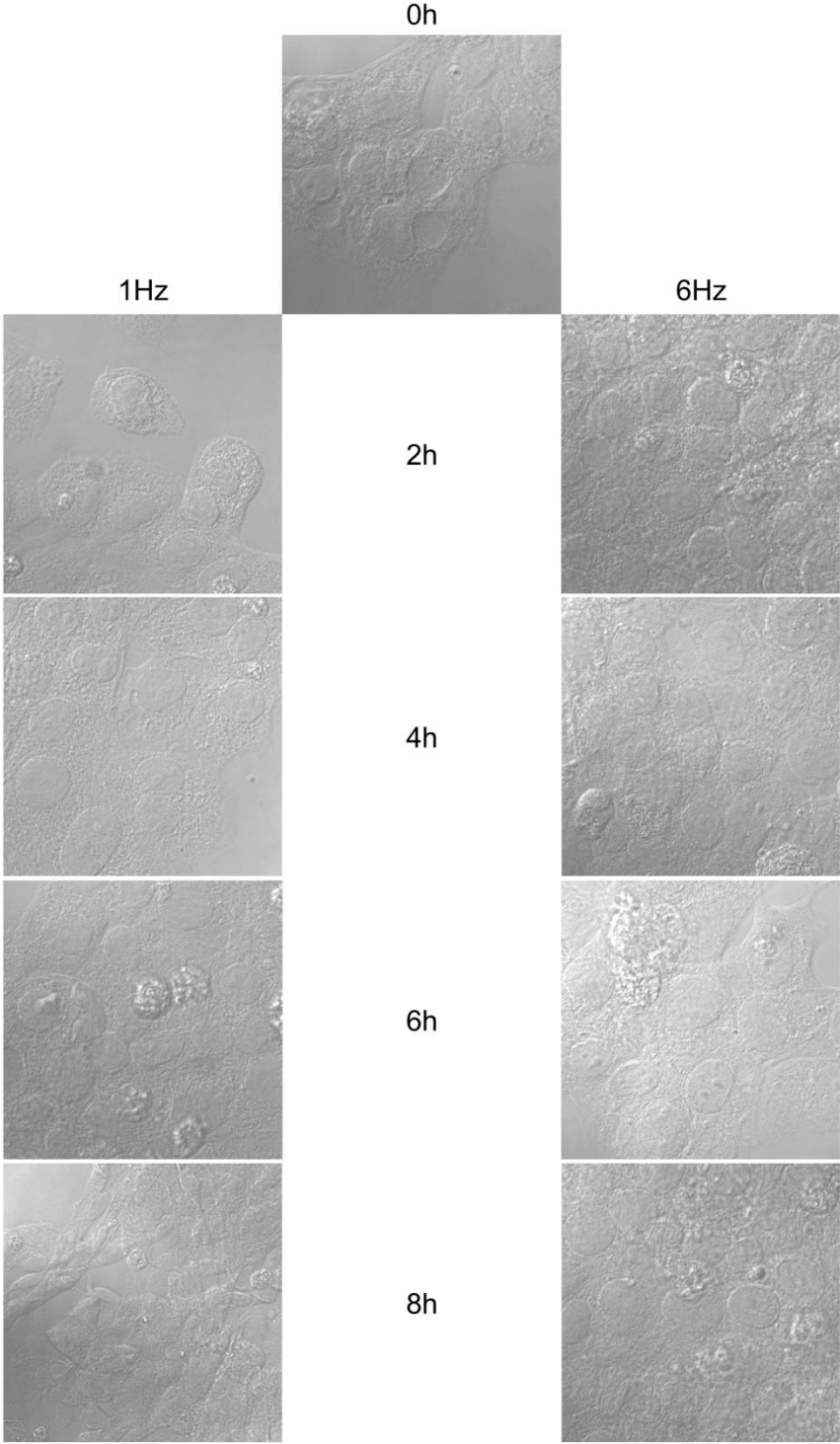
# **Supplemental Material**

**Figure S1. Normal pacing does not change protein expression.**



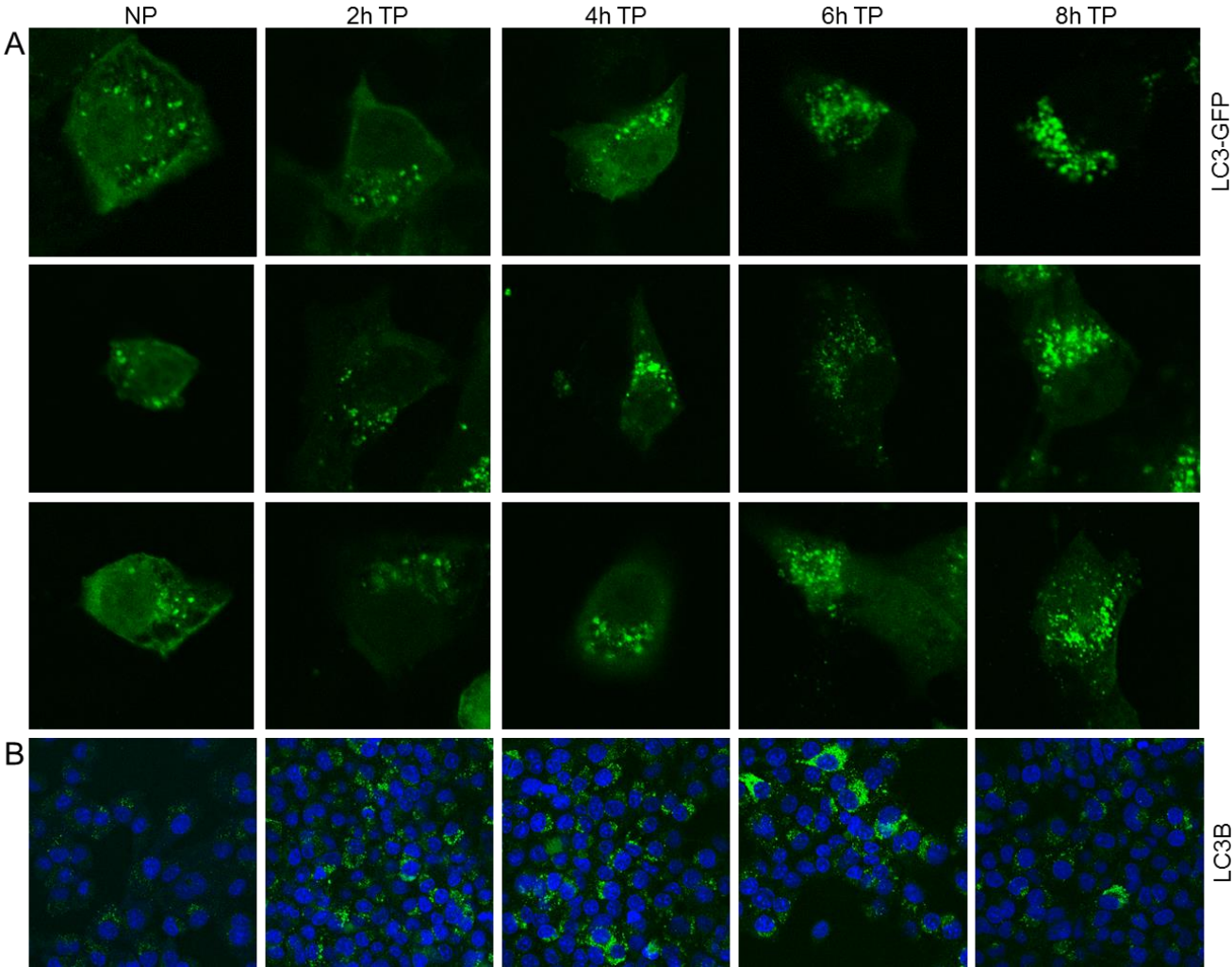
Representative Western blot showing LC3B-I/II, p62, eIF2α-P<sub>S51</sub> and mTOR-P<sub>S2481</sub> expression in normal paced HL-1 cardiomyocytes. Normal pacing does not change the protein expression levels of any of these proteins.

**Figure S2. Normal pacing and tachypacing does not change cardiomyocyte morphology.**



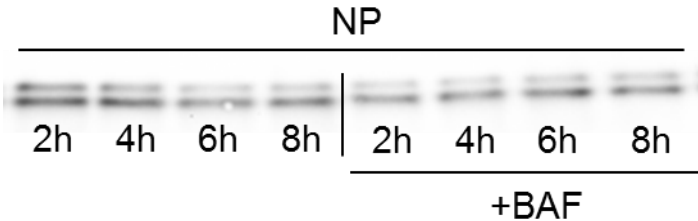
Bright field microscopic images showing the morphology of the HL-1 atrial cardiomyocytes after non-pacing (0 h), normal pacing (1 Hz) or tachypacing (6 Hz). No morphological changes were observed between the conditions as indicated.

**Figure S3. Tachypacing induces autophagosome formation.**



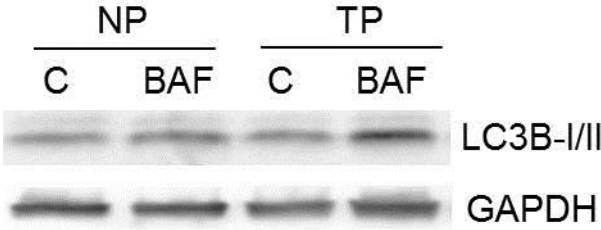
Confocal images of multiple tachypaced HL-1 cardiomyocytes, for the period as indicated, (A) transfected with LC3B-GFP or (B) endogenous LC3B visualized by immunostaining. Green puncta indicate autophagosomes.

**Figure S4. LC3B-II levels are not increased during normal pacing after BAF treatment.**



Representative Western blot showing LC3B-I/II expression in normal paced HL-1 cardiomyocytes with and without BAF treatment. BAF doesn't increase the LC3B-II levels during normal pacing.

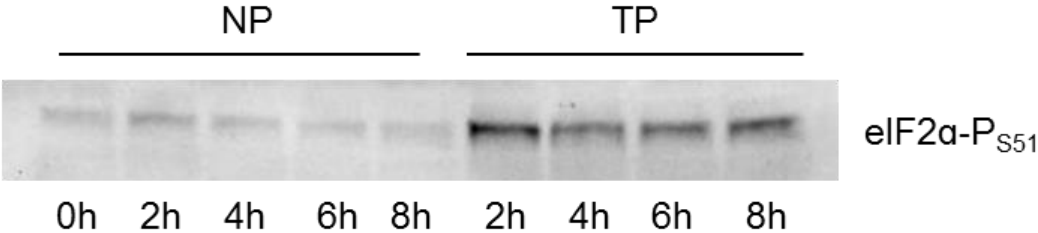
**Figure S5. BAF treatment further increases LC3B-II levels in tachypaced HL-1 cardiomyocytes.**



Representative Western blot showing LC3B-I/II expression in normal paced (NP) and 8 h tachypaced (TP) HL-1 cardiomyocytes with and without BAF treatment. BAF increases the LC3B-II levels after 8h tachypacing.

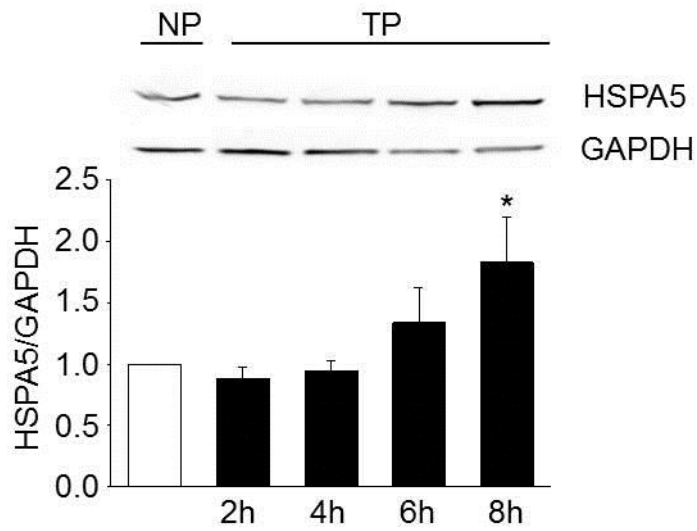


**Figure S6. Normal pacing does not change eIF2α phosphorylation.**



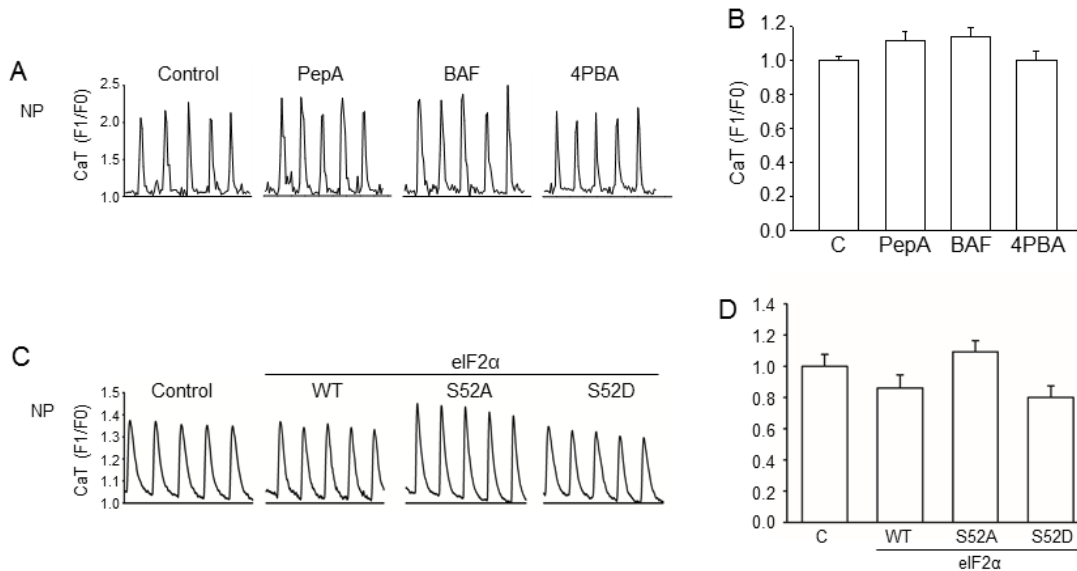
Representative Western blot showing eIF2α phosphorylation in normal paced (NP) and tachypaced (TP) HL-1 cardiomyocytes.

**Figure S7. Tachypacing induces expression of the ER chaperone HSPA5.**



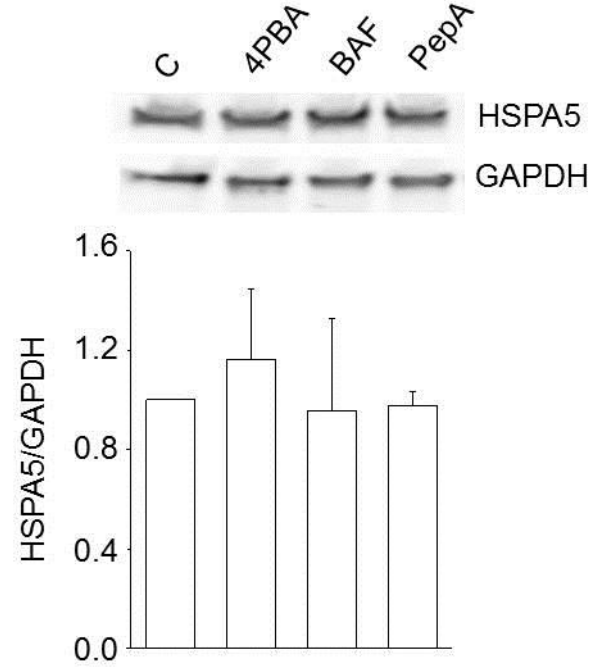
Top panel: representative Western blot showing HSPA5 and GAPDH expression in normal paced (NP) and tachypaced (TP) HL-1 cardiomyocytes. Bottom: quantified data revealing significant increase in HSPA5 levels in tachypaced HL-1 cardiomyocytes (N=3). \* $P \leq 0.05$  vs NP.

**Figures S8. The effect of pharmacological and genetic modulation of autophagy and ER stress in normal paced and tachypaced HL-1 cardiomyocytes.**



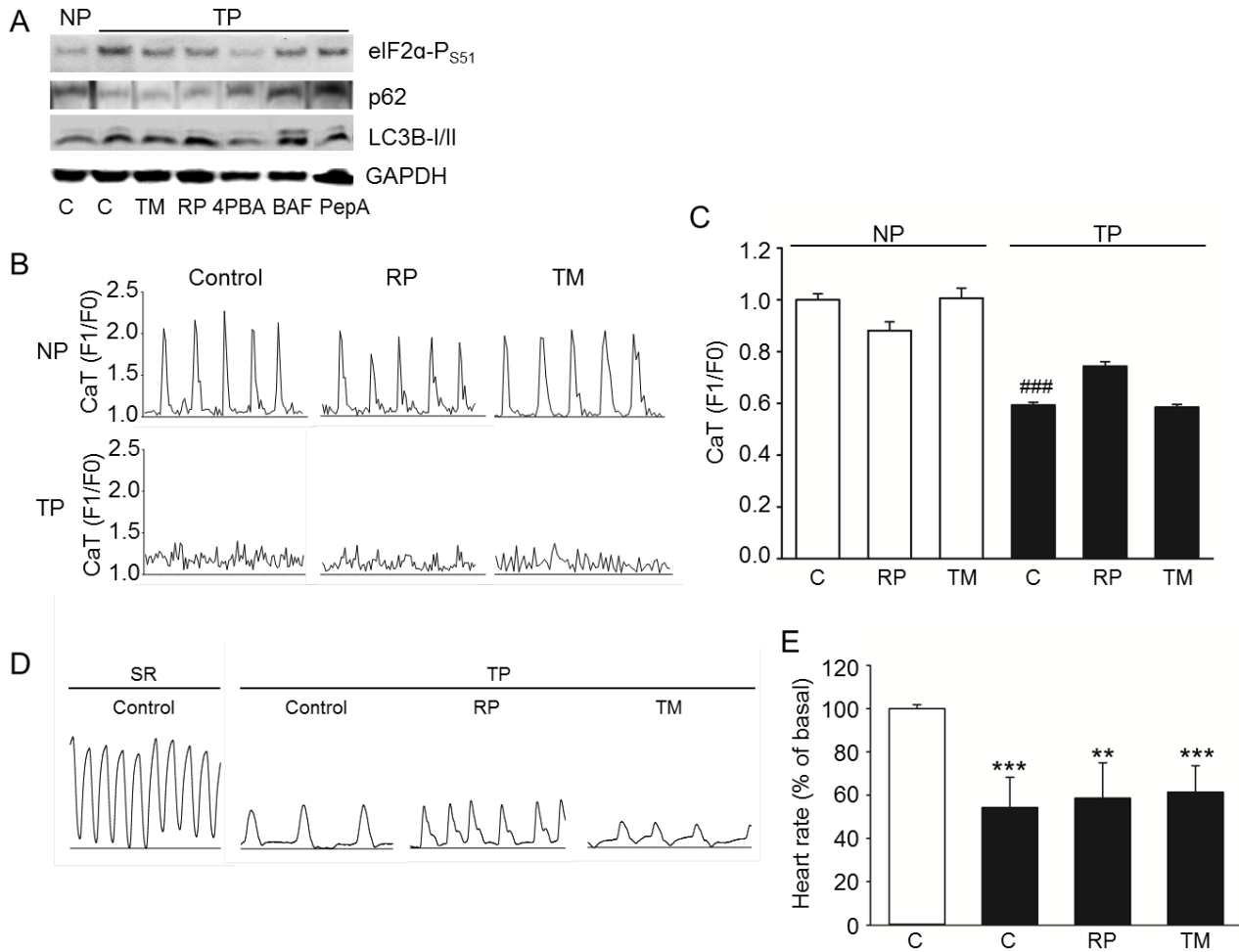
**(A)** Representative CaT (5 sec) of HL-1 cardiomyocytes after normal pacing (NP). HL-1 cardiomyocytes were pre-treated with the autophagy modulators PepA or BAF, or the chemical chaperone 4PBA, followed by normal and measurement of CaT. **(B)** Quantified CaT of HL-1 cardiomyocytes pretreated with pepstatin A, bafilomycin A1 or 4PBA and subjected to normal pacing, which does not change calcium transients (n/N=60/4). **(C)** Representative CaT (5 sec) of HL-1 cardiomyocytes transfected with empty plasmid (Control), eIF2α wild-type, non-phosphorylated (S52A) or phospho-mimetic (S52D) mutant and followed by NP. **(D)** Quantified CaT of HL-1 cardiomyocytes transiently transfected with empty plasmid (Control), eIF2α wild-type, non-phosphorylated (S52A) or phospho-mimetic (S52D) mutant and subjected to normal pacing, which does not change calcium transients (n/N=30/3).

**Figure S9. Pharmacological modulation of autophagy in HL-1 cardiomyocytes does not change HSPA5 expression.**



Top panel: representative Western blot showing HSPA5 and GAPDH levels in HL-1 cardiomyocytes pretreated with various autophagy modulators as indicated. Lower panel: quantified data showing no significant changes in HSPA5 levels for the conditions as indicated (N=3).

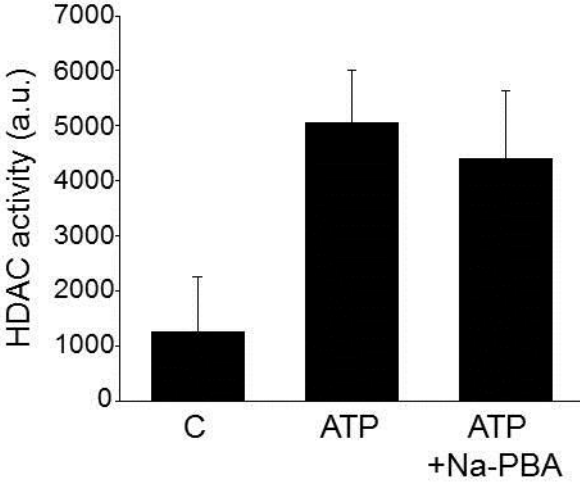
**Figure S10. Activators of ER stress and autophagy do not protect against tachypacing-induced contractile dysfunction in HL-1 cardiomyocytes and *Drosophila*.**



**(A)** Representative Western blot showing eIF2 $\alpha$ -P<sub>S51</sub>, p62, LC3B-I/II and GAPDH levels in HL-1 cardiomyocytes pretreated with the ER stress-inducer tunicamycin (TM), the autophagy-inducer rapamycin (RP), autophagy inhibitors BAF and pepstatin A and the chemical chaperone 4PBA. RP and TM show no protection against tachypacing-induced changes in eIF2 $\alpha$ -P<sub>S51</sub>, p62 or LC3B-I/II expression. **(B)** Representative CaT of HL-1 cardiomyocytes after normal pacing (NP) or tachypacing (TP), pre-treated with TM or RP. **(C)** Quantified CaT amplitude of NP and TP HL-1 cardiomyocytes, each from groups as indicated (n/N=50/3). There is no significant decrease in CaT amplitude for either RP or TM at NP, due to the non-toxic concentrations applied.

Nevertheless, RP and TM did not protect against contractile dysfunction. **(D)** Representative heart wall contractions of *Drosophila* monitored before TP and after TP with DMSO (Control), TM or RP pretreatment. **(E)** Quantified data showing heart wall contraction rates from groups as indicated. RP and TM did not protect against contractile dysfunction. White bars represent normal paced (NP in HL-1 cardiomyocytes) or spontaneous heart rate (SR in *Drosophila*) and black bars represent tachypaced HL-1 cardiomyocytes or *Drosophila*. N=9 to 15 prepupae for each group. \*\* $P \leq 0.01$ , \*\*\* $P \leq 0.001$  vs control SR, ### $P \leq 0.001$  vs control TP

**Figure S11. 4PBA has no effect on HDAC activity in dogs.**



Atrial tachypacing of dogs results in a borderline significant induction ( $P=0.06$ ) of HDAC activity, which was not altered by 4PBA treatment ( $N= 7$  dogs for each group).

### **Supplemental Video Legends:**

**Video S1.** Time-lapse video shows CaT after 8 hours normal pacing (1Hz) of HL-1 cardiomyocytes. Images were acquired at 2 ms intervals.

**Video S2.** Time-lapse video shows CaT after 8 hours tachypacing (6Hz) of HL-1 cardiomyocytes. Images were acquired at 2 ms intervals.

**Video S3.** Time-lapse video shows CaT after 8 hours tachypacing (1Hz) of HL-1 cardiomyocytes pretreated with 4PBA. Images were acquired at 2 ms intervals.

**Video S4.** Time-lapse video shows CaT after 8 hours tachypacing (6Hz) of HL-1 cardiomyocytes pretreated with 4PBA. Images were acquired at 2 ms intervals.

**Video S5.** Time-lapse video shows CaT after 8 hours tachypacing (1Hz) of HL-1 cardiomyocytes transfected with empty plasmid. Images were acquired at 2 ms intervals.

**Video S6.** Time-lapse video shows CaT after 8 hours tachypacing (6Hz) of HL-1 cardiomyocytes transfected with empty plasmid. Images were acquired at 2 ms intervals.

**Video S7.** Time-lapse video shows CaT after 8 hours tachypacing (1Hz) of HL-1 cardiomyocytes transfected with HSPA5 construct. Images were acquired at 2 ms intervals.

**Video S8.** Time-lapse video shows CaT after 8 hours tachypacing (6Hz) of HL-1 cardiomyocytes transfected with HSPA5 construct. Images were acquired at 2 ms intervals.



**Video S9.** Time-lapse video shows CaT after 8 hours tachypacing (1Hz) of HL-1 cardiomyocytes pretreated with pepstatin A. Images were acquired at 2 ms intervals.

**Video S10.** Time-lapse video shows CaT after 8 hours tachypacing (6Hz) of HL-1 cardiomyocytes pretreated with pepstatin A. Images were acquired at 2 ms intervals.

**Video S11.** Time-lapse video shows CaT after 8 hours tachypacing (1Hz) of HL-1 cardiomyocytes pretreated with BAF. Images were acquired at 2 ms intervals.

**Video S12.** Time-lapse video shows CaT after 8 hours tachypacing (6Hz) of HL-1 cardiomyocytes pretreated with BAF. Images were acquired at 2 ms intervals.

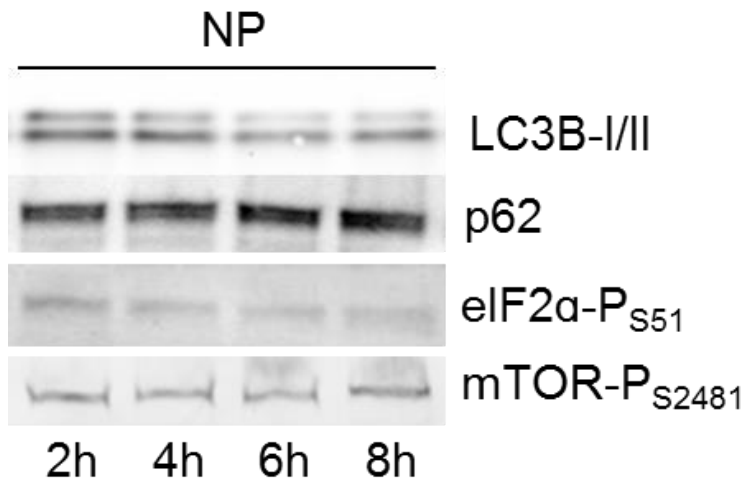
**Video S13.** Time-lapse video shows heart wall contractions of a prepupae of a W1118 genetic background before tachypacing, and after tachypacing (5Hz, **Video S14**).

**Video S15.** Time-lapse video shows heart wall contractions of a prepupae of a W1118 genetic background pretreated with BAF before tachypacing, and after tachypacing (5Hz, **Video S16**).

**Video S17.** Time-lapse video shows heart wall contractions of a prepupae of a W1118 genetic background pretreated with 4PBA before tachypacing, and after tachypacing (5Hz, **Video S18**).

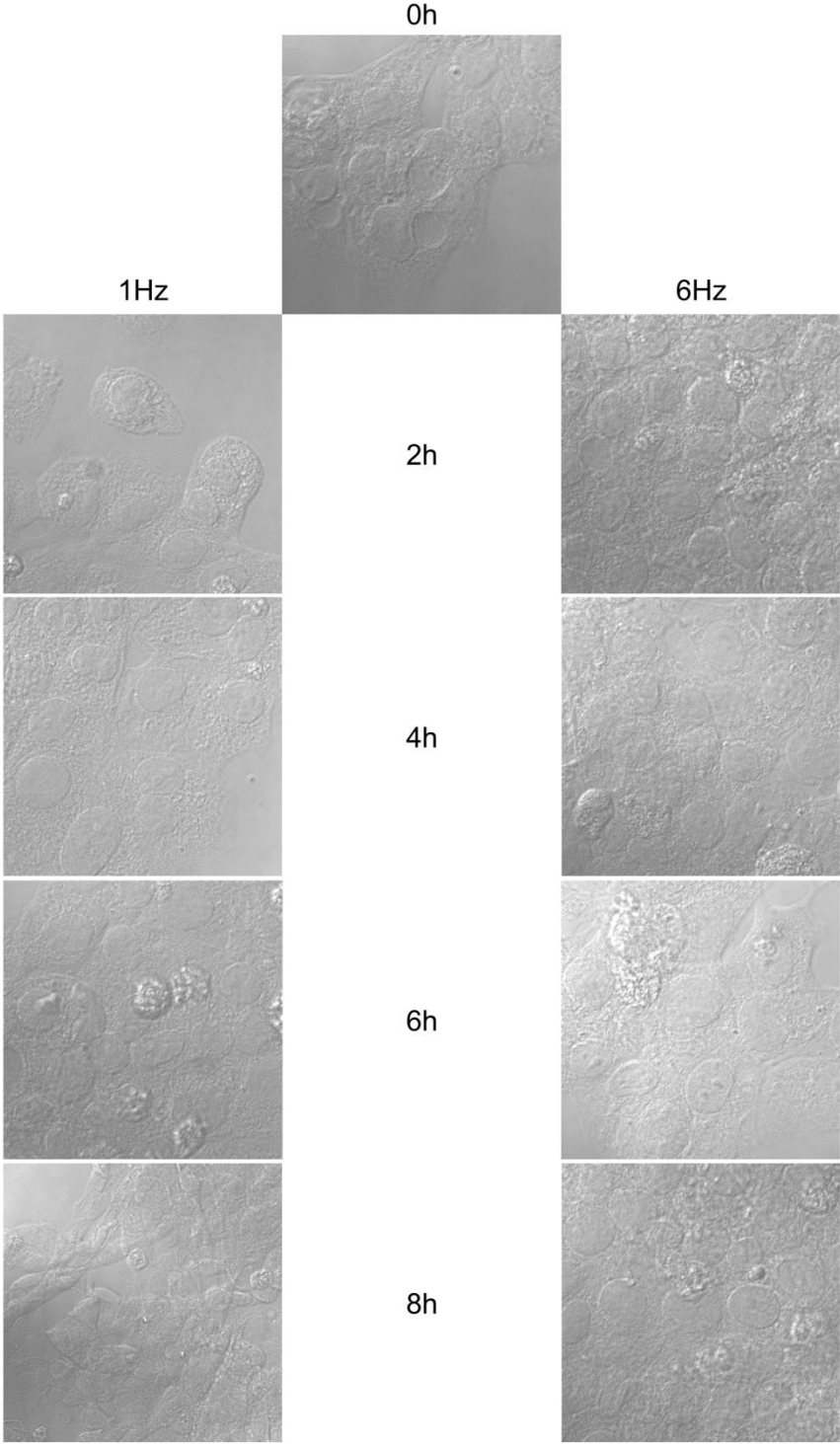
# **Supplemental Material**

**Figure S1. Normal pacing does not change protein expression.**



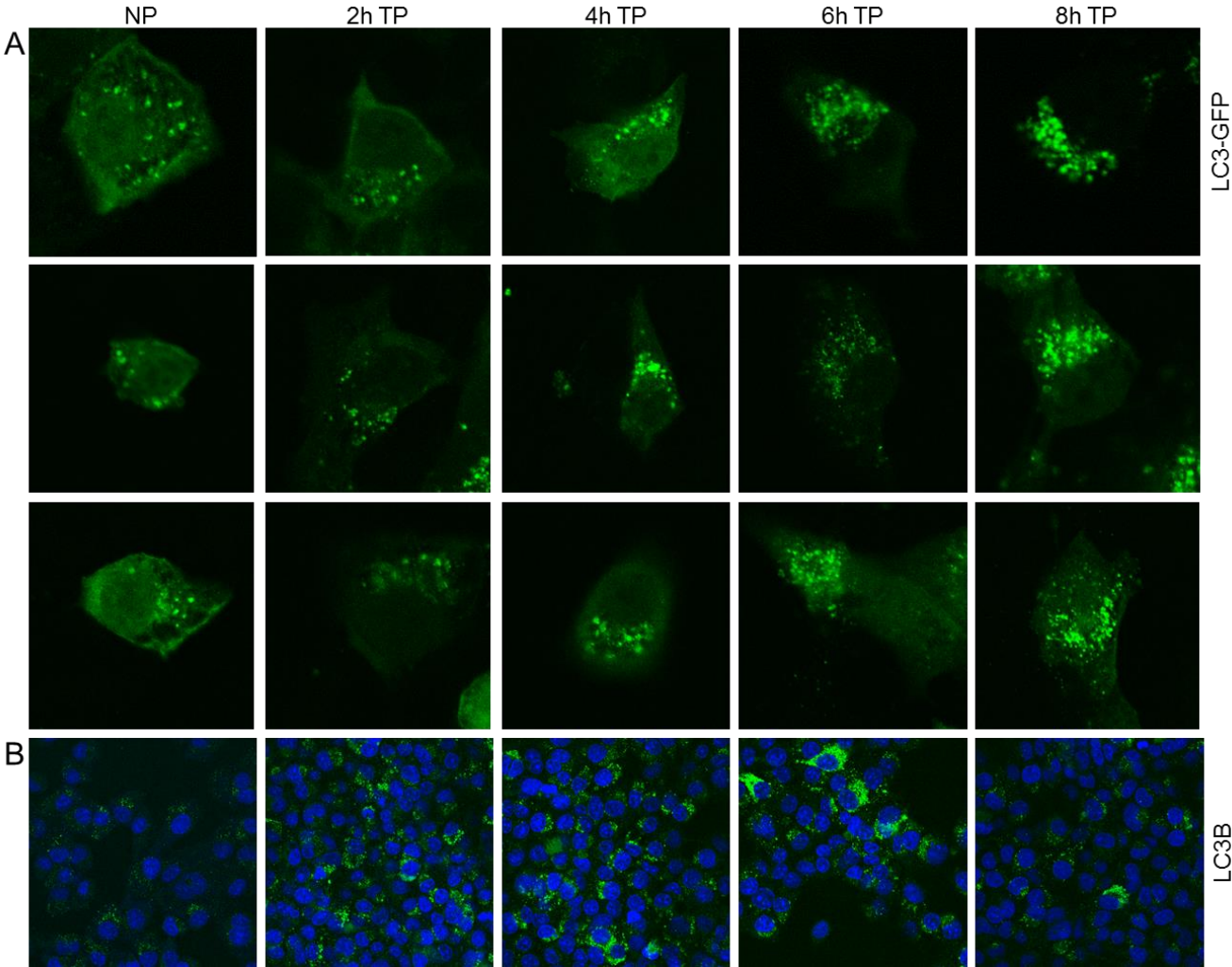
Representative Western blot showing LC3B-I/II, p62, eIF2α-P<sub>S51</sub> and mTOR-P<sub>S2481</sub> expression in normal paced HL-1 cardiomyocytes. Normal pacing does not change the protein expression levels of any of these proteins.

**Figure S2. Normal pacing and tachypacing does not change cardiomyocyte morphology.**



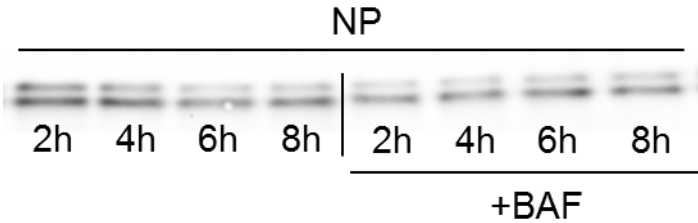
Bright field microscopic images showing the morphology of the HL-1 atrial cardiomyocytes after non-pacing (0 h), normal pacing (1 Hz) or tachypacing (6 Hz). No morphological changes were observed between the conditions as indicated.

**Figure S3. Tachypacing induces autophagosome formation.**



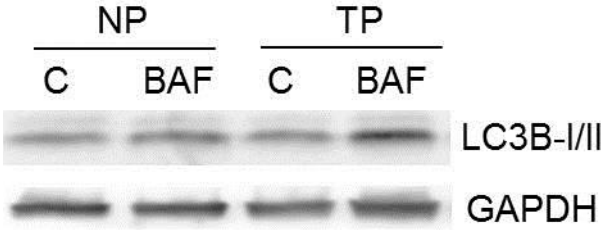
Confocal images of multiple tachypaced HL-1 cardiomyocytes, for the period as indicated, (A) transfected with LC3B-GFP or (B) endogenous LC3B visualized by immunostaining. Green puncta indicate autophagosomes.

**Figure S4. LC3B-II levels are not increased during normal pacing after BAF treatment.**



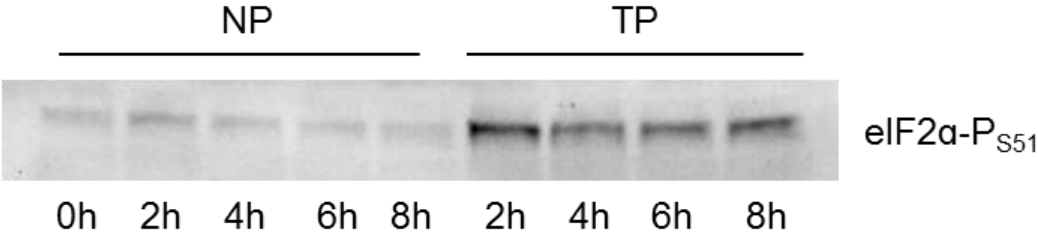
Representative Western blot showing LC3B-I/II expression in normal paced HL-1 cardiomyocytes with and without BAF treatment. BAF doesn't increase the LC3B-II levels during normal pacing.

**Figure S5. BAF treatment further increases LC3B-II levels in tachypaced HL-1 cardiomyocytes.**



Representative Western blot showing LC3B-I/II expression in normal paced (NP) and 8 h tachypaced (TP) HL-1 cardiomyocytes with and without BAF treatment. BAF increases the LC3B-II levels after 8h tachypacing.

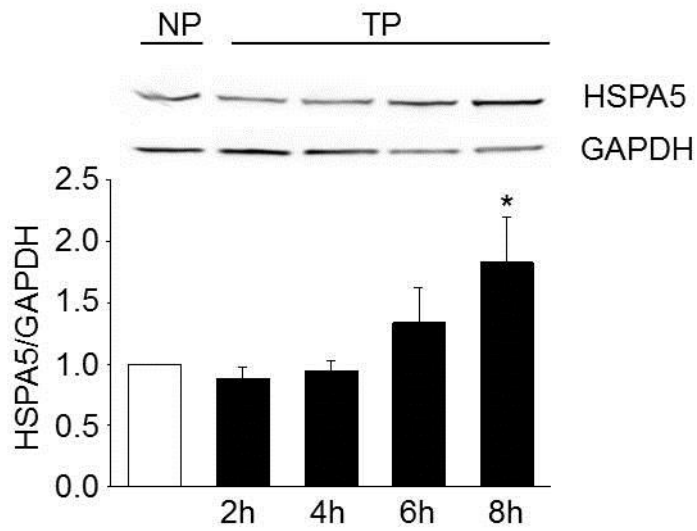
**Figure S6. Normal pacing does not change eIF2α phosphorylation.**



Representative Western blot showing eIF2α phosphorylation in normal paced (NP) and tachypaced (TP) HL-1 cardiomyocytes.

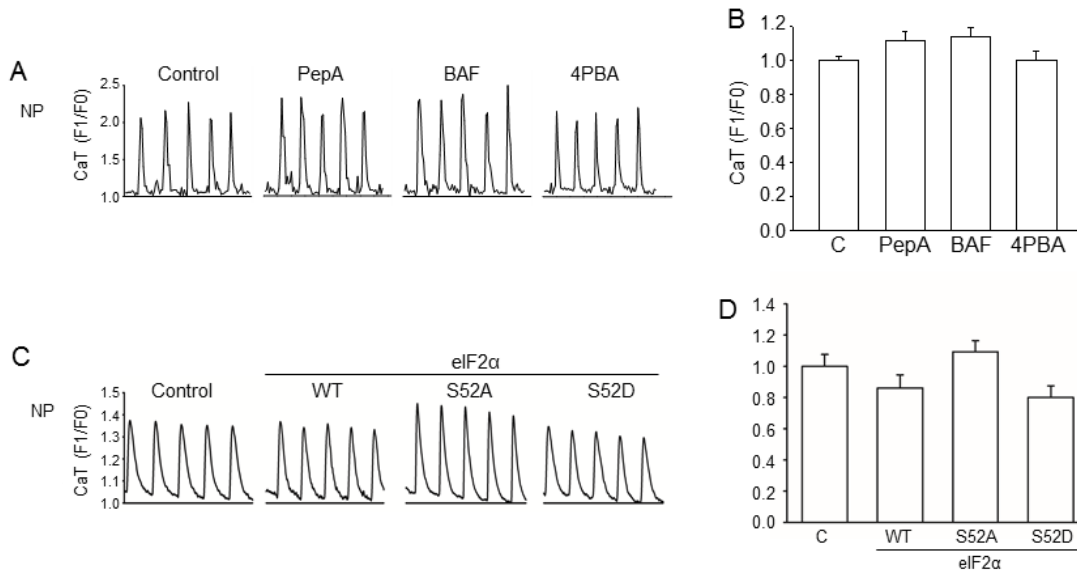


**Figure S7. Tachypacing induces expression of the ER chaperone HSPA5.**



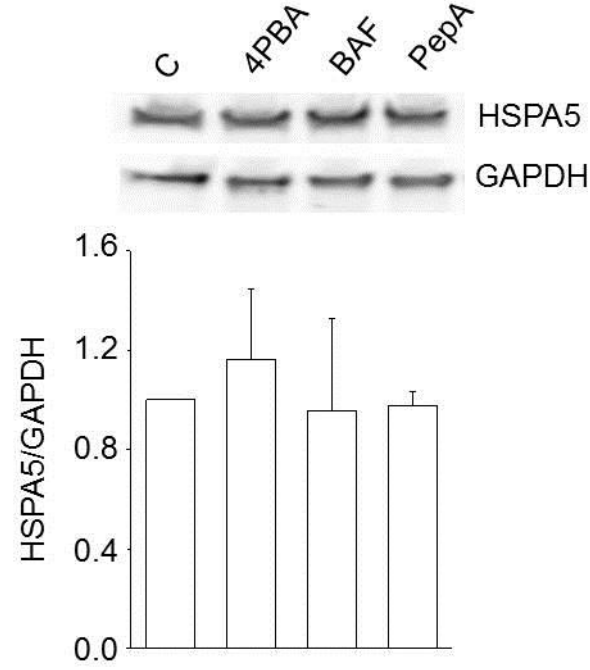
Top panel: representative Western blot showing HSPA5 and GAPDH expression in normal paced (NP) and tachypaced (TP) HL-1 cardiomyocytes. Bottom: quantified data revealing significant increase in HSPA5 levels in tachypaced HL-1 cardiomyocytes (N=3). \* $P \leq 0.05$  vs NP.

**Figures S8. The effect of pharmacological and genetic modulation of autophagy and ER stress in normal paced and tachypaced HL-1 cardiomyocytes.**



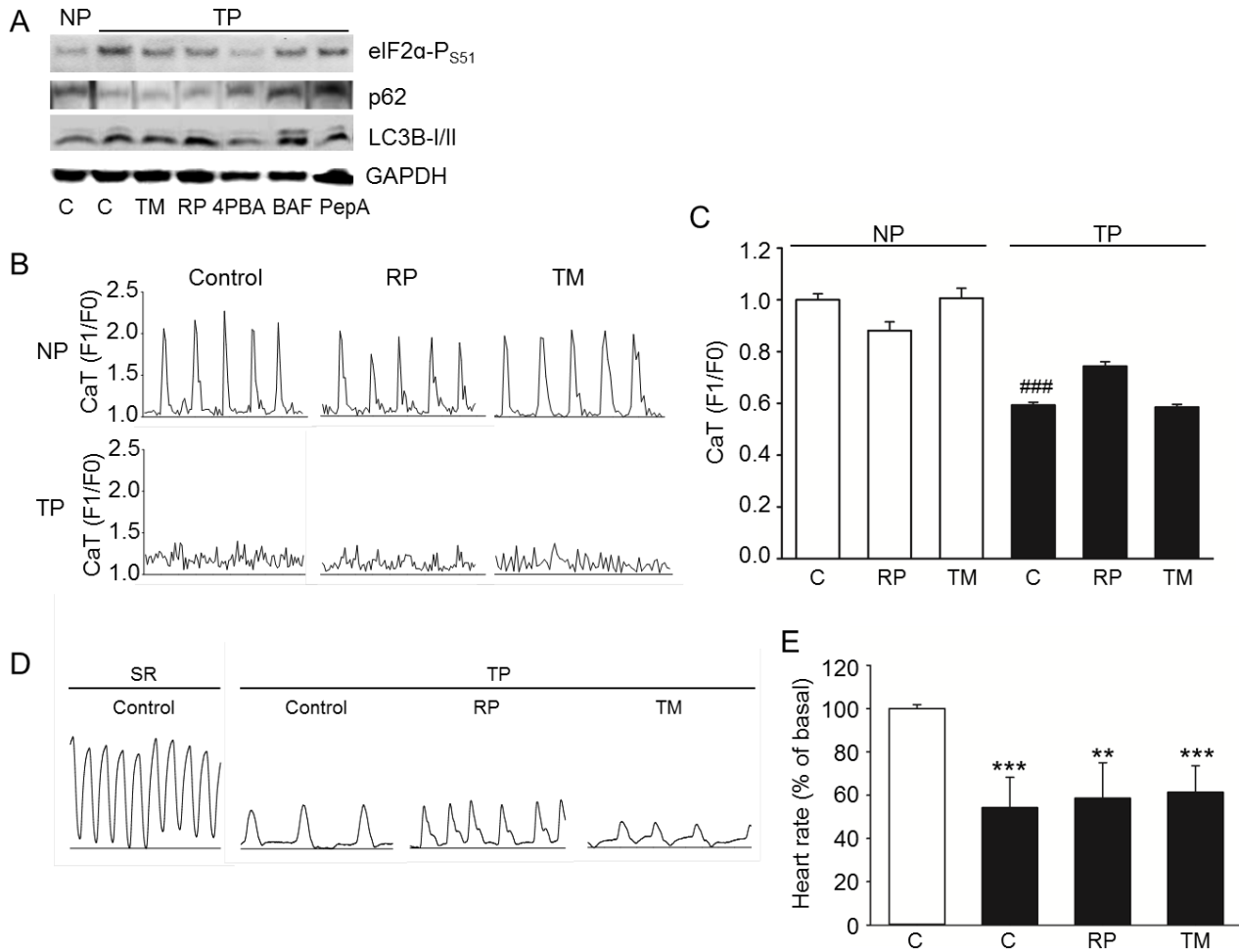
**(A)** Representative CaT (5 sec) of HL-1 cardiomyocytes after normal pacing (NP). HL-1 cardiomyocytes were pre-treated with the autophagy modulators PepA or BAF, or the chemical chaperone 4PBA, followed by normal and measurement of CaT. **(B)** Quantified CaT of HL-1 cardiomyocytes pretreated with pepstatin A, bafilomycin A1 or 4PBA and subjected to normal pacing, which does not change calcium transients (n/N=60/4). **(C)** Representative CaT (5 sec) of HL-1 cardiomyocytes transfected with empty plasmid (Control), eIF2α wild-type, non-phosphorylated (S52A) or phospho-mimetic (S52D) mutant and followed by NP. **(D)** Quantified CaT of HL-1 cardiomyocytes transiently transfected with empty plasmid (Control), eIF2α wild-type, non-phosphorylated (S52A) or phospho-mimetic (S52D) mutant and subjected to normal pacing, which does not change calcium transients (n/N=30/3).

**Figure S9. Pharmacological modulation of autophagy in HL-1 cardiomyocytes does not change HSPA5 expression.**



Top panel: representative Western blot showing HSPA5 and GAPDH levels in HL-1 cardiomyocytes pretreated with various autophagy modulators as indicated. Lower panel: quantified data showing no significant changes in HSPA5 levels for the conditions as indicated (N=3).

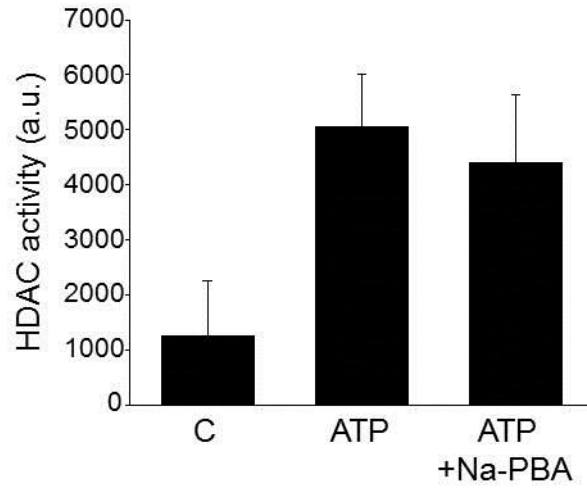
**Figure S10. Activators of ER stress and autophagy do not protect against tachypacing-induced contractile dysfunction in HL-1 cardiomyocytes and *Drosophila*.**



**(A)** Representative Western blot showing eIF2 $\alpha$ -P<sub>S51</sub>, p62, LC3B-I/II and GAPDH levels in HL-1 cardiomyocytes pretreated with the ER stress-inducer tunicamycin (TM), the autophagy-inducer rapamycin (RP), autophagy inhibitors BAF and pepstatin A and the chemical chaperone 4PBA. RP and TM show no protection against tachypacing-induced changes in eIF2 $\alpha$ -P<sub>S51</sub>, p62 or LC3B-I/II expression. **(B)** Representative CaT of HL-1 cardiomyocytes after normal pacing (NP) or tachypacing (TP), pre-treated with TM or RP. **(C)** Quantified CaT amplitude of NP and TP HL-1 cardiomyocytes, each from groups as indicated (n/N=50/3). There is no significant decrease in CaT amplitude for either RP or TM at NP, due to the non-toxic concentrations applied.

Nevertheless, RP and TM did not protect against contractile dysfunction. **(D)** Representative heart wall contractions of *Drosophila* monitored before TP and after TP with DMSO (Control), TM or RP pretreatment. **(E)** Quantified data showing heart wall contraction rates from groups as indicated. RP and TM did not protect against contractile dysfunction. White bars represent normal paced (NP in HL-1 cardiomyocytes) or spontaneous heart rate (SR in *Drosophila*) and black bars represent tachypaced HL-1 cardiomyocytes or *Drosophila*. N=9 to 15 prepupae for each group. \*\* $P \leq 0.01$ , \*\*\* $P \leq 0.001$  vs control SR, ### $P \leq 0.001$  vs control TP

**Figure S11. 4PBA has no effect on HDAC activity in dogs.**



Atrial tachypacing of dogs results in a borderline significant induction ( $P=0.06$ ) of HDAC activity, which was not altered by 4PBA treatment (N= 7 dogs for each group).

### **Supplemental Video Legends:**

**Video S1.** Time-lapse video shows CaT after 8 hours normal pacing (1Hz) of HL-1 cardiomyocytes. Images were acquired at 2 ms intervals.

**Video S2.** Time-lapse video shows CaT after 8 hours tachypacing (6Hz) of HL-1 cardiomyocytes. Images were acquired at 2 ms intervals.

**Video S3.** Time-lapse video shows CaT after 8 hours tachypacing (1Hz) of HL-1 cardiomyocytes pretreated with 4PBA. Images were acquired at 2 ms intervals.

**Video S4.** Time-lapse video shows CaT after 8 hours tachypacing (6Hz) of HL-1 cardiomyocytes pretreated with 4PBA. Images were acquired at 2 ms intervals.

**Video S5.** Time-lapse video shows CaT after 8 hours tachypacing (1Hz) of HL-1 cardiomyocytes transfected with empty plasmid. Images were acquired at 2 ms intervals.

**Video S6.** Time-lapse video shows CaT after 8 hours tachypacing (6Hz) of HL-1 cardiomyocytes transfected with empty plasmid. Images were acquired at 2 ms intervals.

**Video S7.** Time-lapse video shows CaT after 8 hours tachypacing (1Hz) of HL-1 cardiomyocytes transfected with HSPA5 construct. Images were acquired at 2 ms intervals.

**Video S8.** Time-lapse video shows CaT after 8 hours tachypacing (6Hz) of HL-1 cardiomyocytes transfected with HSPA5 construct. Images were acquired at 2 ms intervals.

**Video S9.** Time-lapse video shows CaT after 8 hours tachypacing (1Hz) of HL-1 cardiomyocytes pretreated with pepstatin A. Images were acquired at 2 ms intervals.

**Video S10.** Time-lapse video shows CaT after 8 hours tachypacing (6Hz) of HL-1 cardiomyocytes pretreated with pepstatin A. Images were acquired at 2 ms intervals.

**Video S11.** Time-lapse video shows CaT after 8 hours tachypacing (1Hz) of HL-1 cardiomyocytes pretreated with BAF. Images were acquired at 2 ms intervals.

**Video S12.** Time-lapse video shows CaT after 8 hours tachypacing (6Hz) of HL-1 cardiomyocytes pretreated with BAF. Images were acquired at 2 ms intervals.

**Video S13.** Time-lapse video shows heart wall contractions of a prepupae of a W1118 genetic background before tachypacing, and after tachypacing (5Hz, **Video S14**).

**Video S15.** Time-lapse video shows heart wall contractions of a prepupae of a W1118 genetic background pretreated with BAF before tachypacing, and after tachypacing (5Hz, **Video S16**).

**Video S17.** Time-lapse video shows heart wall contractions of a prepupae of a W1118 genetic background pretreated with 4PBA before tachypacing, and after tachypacing (5Hz, **Video S18**).